Nuclear Phosphatidylinositol 3,4,5-Trisphosphate Interactome Uncovers an Enrichment in Nucleolar Proteins

Authors

Fatemeh Mazloumi Gavgani, Malene Skuseth Slinning, Andrea Papdiné Morovicz, Victoria Smith Arnesen, Diana C. Turcu, Sandra Ninzima, Clive S. D'Santos, and Aurélia E. Lewis

Correspondence

aurelia.lewis@uib.no

Graphical Abstract

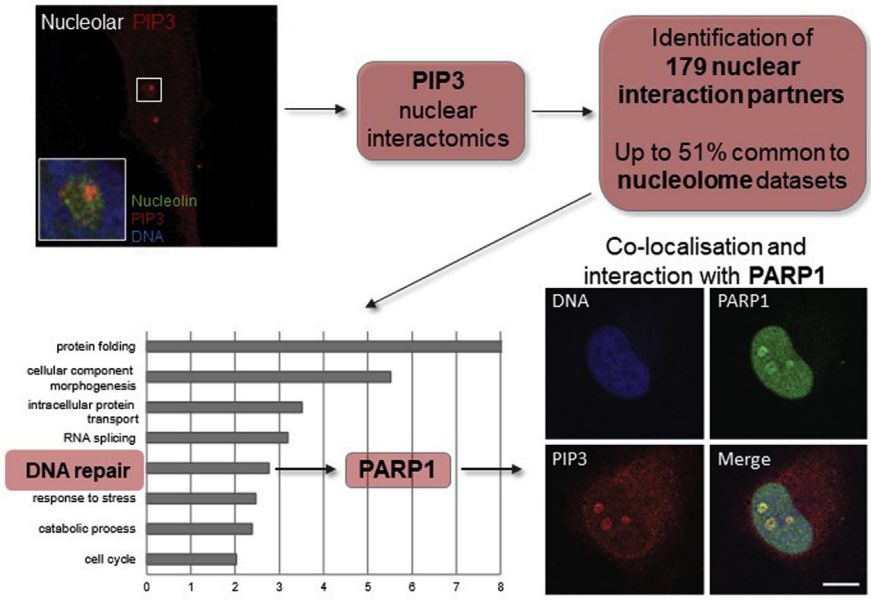

In Brief

The polyphosphoinositide (PPIn) phosphatidylinositol 3,4,5 trisphosphate (PtdIns(3,4,5)P_3) localizes to the nucleus and nucleolus. Using an affinity enrichment MS approach, the nuclear PtdIns(3,4,5)P_3 interactome identified new interaction partners associated with the nucleolus. Among these, the DNA repair PARP1 protein, colocalized to the nucleolus with PtdIns(3,4,5)P_3 and showed direct interaction to PPIn *via* three polybasic regions. The nuclear PtdIns(3,4,5)P_3 interactome reported here will serve as a resource to further investigate the molecular mechanisms underlying PtdIns(3,4,5)P_3-mediated interactions in the nucleus and nucleolus.

Highlights

- Phosphatidylinositol 3,4,5-trisphosphate (PtdIns(3,4,5)P_3) localizes to nucleoli.
- PtdIns(3,4,5)P_3 interactomics from isolated nuclei identifies nucleolar proteins.
- PARP1 interacts directly with polyphosphoinositides *via* several polybasic regions.
- PARP1 colocalizes with PtdIns(3,4,5)P_3 in the nucleolus.

2021, Mol Cell Proteomics *20*, 100102

https://doi.org/10.1016/j.mcpro.2021.100102

Nuclear Phosphatidylinositol 3,4,5-Trisphosphate Interactome Uncovers an Enrichment in Nucleolar Proteins

Fatemeh Mazloumi Gavgani[1], Malene Skuseth Slinning[1], Andrea Papdiné Morovicz[1], Victoria Smith Arnesen[1], Diana C. Turcu[1], Sandra Ninzima[1], Clive S. D'Santos[2], and Aurélia E. Lewis[1,*]

Polyphosphoinositides (PPIns) play essential roles as lipid signaling molecules, and many of their functions have been elucidated in the cytoplasm. However, PPIns are also intranuclear where they contribute to chromatin remodeling, transcription, and mRNA splicing. The PPIn, phosphatidylinositol 3,4,5-trisphosphate (PtdIns(3,4,5)P_3), has been mapped to the nucleus and nucleoli, but its role remains unclear in this subcellular compartment. To gain further insights into the nuclear functions of PtdIns(3,4,5)P_3, we applied a previously developed quantitative MS-based approach to identify the targets of PtdIns(3,4,5)P_3 from isolated nuclei. We identified 179 potential PtdIns(3,4,5)P_3-interacting partners, and gene ontology analysis for the biological functions of this dataset revealed an enrichment in RNA processing/splicing, cytokinesis, protein folding, and DNA repair. Interestingly, about half of these interactors were common to nucleolar protein datasets, some of which had dual functions in rRNA processes and DNA repair, including poly(ADP-ribose) polymerase 1 (PARP1, now referred as ADP-ribosyltransferase 1). PARP1 was found to interact directly with PPIn *via* three polybasic regions in the DNA-binding domain and the linker located N-terminal of the catalytic region. PARP1 was shown to bind to PtdIns(3,4,5)P_3 as well as phosphatidylinositol 3,4-bisphosphate *in vitro* and to colocalize with PtdIns(3,4,5)P_3 in the nucleolus and with phosphatidylinositol 3,4-bisphosphate in nucleoplasmic foci. In conclusion, the PtdIns(3,4,5)P_3 interactome reported here will serve as a resource to further investigate the molecular mechanisms underlying PtdIns(3,4,5)P_3-mediated interactions in the nucleus and nucleolus.

Polyphosphoinositides (PPIns, nomenclature from Michell *et al.* (1)) are phosphorylated derivatives of the glycerophospholipid, phosphatidylinositol (PtdIns) (2). The inositol ring can be reversibly phosphorylated at the 3', 4', and 5' hydroxyl groups, producing seven different PPIns, that is, phosphatidylinositol 3-phosphate, phosphatidylinositol 4-phosphate (PtdIns4*P*), and phosphatidylinositol 5-phosphate, phosphatidylinositol 3,4-bisphosphate (PtdIns(3,4)P_2), phosphatidylinositol 3,5-bisphosphate, phosphatidylinositol 4,5-bisphosphate (PtdIns(4,5)P_2), and phosphatidylinositol 3,4,5-trisphosphate (PtdIns(3,4,5)P_3) (3). These lipids can act directly as signaling molecules or indirectly as precursors of second messengers. They are metabolized in different subcellular compartments because of the presence of substrate-specific PPIn-metabolizing kinases and phosphatases (4, 5). While the roles and regulation of PPIn have been extensively studied in the cytoplasm, the importance of their nuclear roles is only recently becoming more apparent (6, 7). The presence of PPIns as well as specific PPIn enzymes was first demonstrated in an intranuclear pool not associated with the nuclear envelop (8, 9). The concept of PPIn metabolism and signaling occurring in the nucleus independently of the cytoplasm was reported shortly after in several studies (10–12). Consequently, with the exception of phosphatidylinositol 3,5-bisphosphate, the remaining six PPIns have been detected and/or quantified in the nucleus (13–28). The intranuclear biophysico-chemical state of PPIns is still unclear, but several possibilities are emerging to explain how the acyl chains can be shielded from the nuclear aqueous environment. These have been shown to be buried in the hydrophobic ligand pocket of the nuclear receptors liver receptor homolog-1 and steroidogenic factor 1, whereas the inositol headgroup remains accessible for modification by PPIn enzymes (29–31). Alternatively, the presence of nuclear lipid droplets has recently been reported in a few studies (32, 33), including the newly discovered nuclear lipid islets, which consist of PtdIns(4,5)P_2 nuclear

From the [1]Department of Biological Sciences, University of Bergen, Bergen, Norway; [2]CRUK Cambridge Institute, Cambridge University, Cambridge, UK
*For correspondence: Aurélia E. Lewis, aurelia.lewis@uib.no.
Present address for Fatemeh Mazloumi Gavgani: The SARS International Centre for Marine Molecular Biology, Bergen 5006, Norway.
Present address for Victoria Smith Arnesen: Department of Biomedicine, University of Bergen, Bergen, Norway.

https://doi.org/10.1016/j.mcpro.2021.100102

aggregates possibly in the form of micelles, hence accommodating the acyl chains facing inward (34).

Several studies have identified multiple nuclear processes attributed to nuclear PPIns, including mRNA processing, splicing and export, chromatin remodeling, transcription, as well as cell cycle progression (35–41). Nuclear PPIns regulate these processes by interacting electrostatically with proteins *via* pleckstrin homology (PH) domain in few cases (42, 43) but mostly *via* polybasic regions (PBRs), also called K/R-rich motifs ((25, 44–55) and recently reviewed in (7)). So far, PtdIns(4,5)P_2 and its metabolizing enzymes and effector proteins have been identified in nuclear speckles, hubs of mRNA processing and export (20, 21, 47, 56, 57). Other nuclear PtdIns(4,5)P_2 effector proteins have roles in chromatin remodeling (58, 59), transcriptional regulation, and protein stability (51, 60, 61). A minor PtdIns(4,5)P_2 pool was also detected in the nucleolus where it plays a role in RNA polymerase I–mediated transcription (13, 21, 62, 63). Monophosphorylated PPIns interact with several histone-binding proteins (44, 52, 54, 64), transcription factors or cofactors (46, 48, 53). PtdIns(3,4,5)P_3 and the class I phosphoinositide 3-kinase (PI3K) catalytic subunit p110β are localized in the nucleoplasm and nucleolus (19, 25, 28, 65, 66). Only a few nuclear PtdIns(3,4,5)P_3 effector proteins have so far been reported and include the PtdIns(3,4,5)P_3-binding protein (43), GTPase L-isoform of PI3K enhancer (42), mRNA export protein THO complex subunit 4 (aka ALY/REF) (47), O-linked N-acetylglucosamine transferase 110-kDa subunit (OGT) (67), as well as the nucleolar proteins nucleophosmin and ErbB3-binding protein 1 (EBP1) (25, 45). Overall, although PtdIns(3,4,5)P_3 is likely to be a key signaling PPIn in the nucleus, its nuclear function remains largely unknown.

To identify proteins interacting specifically with PtdIns(3,4,5)P_3, several interactomics studies have, so far, been performed from a variety of cell types using either cytosolic (68–70) or whole-cell extract (71). To enrich for nuclear PPIn-interacting proteins, we developed a PPIn quantitative interactomics approach using isolated nuclei and combined with a neomycin-based enrichment of PPIn interactors (49). This approach led to the identification of PtdIns(4,5)P_2 nuclear interacting partners involved in mRNA transcription regulation and mRNA splicing and protein folding. In this study, we have performed quantitative MS-based PtdIns(3,4,5)P_3 interactomics from isolated HeLa nuclei using the same approach (49). We identified 179 potential PtdIns(3,4,5)P_3 protein interactors with functions highly enriched in protein folding, RNA splicing, DNA repair, and cell cycle regulation. Interestingly, half of these proteins were common to the T cell nucleome protein dataset (72). In this study, we focused on poly(ADP-ribose) polymerase 1 (PARP1, now referred as ADP-ribosyltransferase 1), validated its direct interaction with PPIn, including PtdIns(3,4,5)P_3, and determined the sites of interaction that consisted of three PBRs. We also showed that PARP1 localized in nucleoli with PtdIns(3,4,5)P_3 but also in nucleoplasmic foci with PtdIns(3,4)P_2. In sum, this study validates our approach to identify globally PPIn-interacting proteins based in the nucleus and represents a resource for further research efforts investigating the role of PtdIns(3,4,5)P_3 in these interactions.

EXPERIMENTAL PROCEDURES

Materials

The PPIn and control beads were from Echelon Biosciences and consist of biotinylated PPIns bound to streptavidin-coated beads. The acyl chains on both the sn-1 and sn-2 positions are made of six carbons, and biotin is conjugated at the methyl end of the sn-1 acyl chain (P-B345a). Control beads (P-B000) consist of streptavidin-coated beads blocked with biotin. Primers and antibodies used in this study are listed in supplemental Tables S1 and S2, respectively.

Plasmids

The pGEX-4T1-EGFP-GRP1-PH construct was obtained from Julien Viaud (INSERM U.1048, France). The mutant K273A was generated by site-directed mutagenesis in this construct using the primers listed in supplemental Table S1. The pGEX-6P-2-PARP1 domain constructs, amino acids 1 to 214, 215 to 371, 372 to 476, 477 to 524, 525 to 656, and 657 to 1014 were from Michael O Hottiger (University of Zurich, Switzerland) (73). The following mutants were generated by site-directed mutagenesis using the primers listed in supplemental Table S1; pGEX-6P-2-PARP1(1–214)-K84A,K86L-K87L; pGEX-6P-2-PARP1(215–371)-Δ221 to 236; pGEX-6P-2-PARP1(215–371)-Δ346 to 352; pGEX-6P-2-PARP1(477–524)-K505A-K506A and pGEX-6P-2-PARP1(477–524)-K505A-K506A,K508L. All mutations were validated by sequencing using ABI Prism BigDye Terminator version 3.1 cycle sequencing kit (Applied Biosystems).

Cell Culture and SILAC Labeling

HeLa cells were grown in Dulbecco's modified Eagle's medium (DMEM) containing 10% fetal bovine serum in 5% CO_2 at 37 °C. For stable isotope labeling with amino acids in cell culture (SILAC) labeling, HeLa S3 cells were grown in heavy ($^{13}C_6$,$^{15}N_2$-labeled lysine and $^{13}C_6$, $^{15}N_4$-labeled arginine) or light (unlabeled amino acids) DMEM (cat# 280001300, Silantes) supplemented with 10% dialyzed fetal bovine serum (cat# 281000900, Silantes). To examine the efficiency of SILAC, the incorporation of heavy amino acids was validated by LC-MS by Dr Bernd Thiede (University of Oslo, Norway).

Nuclear Fractionation

Cells were grown in 10 × 15 cm (for MS) or in 2 × 10 cm (for Western) plates to about 70% confluency. One hour after adding the fresh medium, the cells were washed with room temperature (RT) PBS, trypsinized, and washed again three times with ice-cold PBS. The cell pellet was resuspended in 5 ml of buffer A (10 mM Hepes, pH 7.9, 1.5 mM $MgCl_2$, 10 mM KCl, 0.5 mM DDT, 1% Igepal, and protease inhibitor cocktail) and incubated on ice for 5 min. The cells were then passed 12 times through a 23-gauge needle to disrupt the cell membrane. The lysates were then centrifuged at 200*g* for 5 min at 4 °C. The supernatant was collected as the cytosolic fraction, and the pellet containing the nuclei was resuspended in 3 ml of buffer S1 (0.25 M sucrose, 10 mM $MgCl_2$, and protease inhibitor cocktail) and layered over 3 ml of buffer S2 (0.35 M sucrose, 0.5 mM $MgCl_2$, and protease inhibitor cocktail) and centrifuged at 1400*g* for 5 min at 4 °C. The nuclear pellets were collected.

Neomycin Extraction

For the PtdIns(3,4,5)P_3 pulldown and MS, nuclei were washed with the retention buffer (20 mM Tris, pH 7.5, 70 mM NaCl, 20 mM KCl, 5 mM $MgCl_2$, 3 mM $CaCl_2$, and protease inhibitor cocktail). The nuclei were then incubated in the retention buffer containing 5 mM neomycin (Neomycin trisulfate salt, Sigma-Aldrich), rotating for 30 min at RT. After centrifugation at 16,000*g* for 5 min, the supernatant containing the neomycin-displaced proteins was collected. Neomycin supernatants were dialysed three times in 900 ml of cold lipid pulldown buffer (20 mM Hepes, pH 7.5, 150 mM NaCl, 5 mM EDTA, and 0.1% Igepal) using Slide-A-Lyzer Mini dialysis units (Thermo Fisher) for 1 h at 4 °C each time. The protein concentration of the dialysed neomycin supernatants was measured using the bicinchoninic acid protein assay (Thermo Fisher Scientific). For Western immunoblotting, nuclei were isolated from 2x 10 cm plates according to Lewis *et al* (49), washed in the retention buffer, divided, and incubated in 60 µl each of the retention buffer in the absence or presence of 5 mM neomycin for 30 min at RT. After centrifugation, supernatants and resulting nuclear pellets were collected.

PPIn Pulldown

PtdIns(3,4,5)P_3 Pulldown for MS—Equal amounts of dialysed neomycin supernatants were used for each pulldown. The heavy extracts were incubated with 100-µl PtdIns(3,4,5)P_3-conjugated bead slurry (P-B345a), and the light extracts were incubated with control beads (P-B000) in lipid pull down buffer (20 mM HEPES pH 7.5, 150 mM NaCl, 5 mM EDTA, 0.1% Igepal) for 1 h rotating at 4 °C. The beads were then washed three times with lipid pulldown buffer containing phosphatase inhibitors (5 mM β-glycerophosphate, 5 mM NaF, and 2 mM Na_3VO_4) and protease inhibitor cocktail. The beads were eluted with 100 µl of 4× LDS sample buffer at 70 °C for 12 min and resolved on two lanes on a Bolt 4 to 12% Bis-Tris gel (Thermo Fisher Scientific) through the stacking gel and proteins were stained with Coomassie Blue.

In Vitro *PPIn Pulldown*—To test the interaction capacity of PPIn-conjugated beads, lipid pulldowns were performed using 1- to 2-µg glutathione S-transferase (GST)-tagged general receptor of phosphoinositides-1(GRP1) or phospholipase C δ1 PH domains and 10 µl of PtdIns(3,4,5)P_3- or PtdIns(4,5)P_2-conjugated bead slurry, respectively, in 400-µl lipid pulldown buffer. 20 µM PtdIns(3,4,5)P_3 diC8 (Echelon P-3908) was used in preincubation. To test the interaction of PARP1 with PPIn, 1.5-µg GST-PARP1 was used together with 15-µl PPIn-conjugated bead slurry.

Proteomics

In-gel Digestion—In-gel trypsin digestion was performed as described (74) with some modifications. Briefly, the Coomassie Brilliant Blue –stained protein bands were excised, and after several washes, the gel pieces were subjected to a reduction step using 10 mM DTT in 100 mM ammonium bicarbonate (NH_4HCO_3) buffer for 45 min at 56 °C. Alkylation was performed with 55 mM iodoacetamide in 100 mM NH_4HCO_3 for 30 min at RT in the dark. Digestion was performed with 10 µl of trypsin (10 mg/l in 50 mM NH_4HCO_3) overnight at 37 °C. Eluted peptides were recovered, and the gel pieces were subsequently washed in 2.5% formic acid/80% acetonitrile for 30 min at 37 °C. The acid wash was combined with the original peptide eluate and dried. Samples were resuspended in 0.1% formic acid and analyzed directly by nano-LC-MS/MS.

Nano-LC-MS/MS—Digested peptide mixtures were analyzed by nano-LC-MS/MS. MS was performed using a Q Exactive HF (Thermo Scientific) coupled to an Ultimate RSLCnano-LC system (Dionex). Optimal separation conditions resulting in maximal peptide coverage were achieved using an Acclaim PepMap 100 column (C18, 3 µm, 100 Å) (Dionex) with an internal diameter of 75 µm and capillary length of 25 cm. A flow rate of 300 nl/min was used with a solvent gradient of 5% B to 45% B in 85 min followed by increasing the gradient to 95% B over 5 min. Solvent A was 0.1% (v/v) formic acid and 5% (v/v) dimethyl sulfoxide in water, whereas the composition of solvent B was 80% (v/v) acetonitrile, 0.1% (v/v) formic acid, and 5% (v/v) dimethyl sulfoxide in water.

The mass spectrometer was operated in positive-ion mode using an N^{th} order double-play method to automatically switch between full-scan acquisition of peptide precursor ions and higher-energy C-trap dissociation-generated fragments both using the Orbitrap mass analyzer. Survey full-scan MS spectra (from 400 to 1600 m/z) were acquired in the Orbitrap with resolution (R) 60,000 at 400 m/z (after accumulation to a target of 3,000,000 charges). The method used allowed sequential isolation of the ten most intense ions for fragmentation, depending on the signal intensity, using higher-energy C-trap dissociation at a target value of 20,000 charges and resolution of 30,000. Target ions already selected for MS/MS were dynamically excluded for 30 s. Unassigned and 1+ charges were excluded from fragmentation selection. General MS conditions were electrospray voltage, 2.5 kV, with no sheath or auxiliary gas flow, an ion selection threshold of 2000 counts for MS/MS, an activation Q value of 0.25, activation time of 12 ms, capillary temperature of 200 °C, and an S-Lens RF level of 60%. Charge state screening was enabled, and precursors with unknown charge state or a charge state of 1 were excluded. Raw MS data files were processed using Proteome Discoverer v.2.1 (Thermo Scientific). Processed files were searched against the human FASTA database (taxon ID 9606–Version February 2017) using the SEQUEST HT search engine. Searches were performed with tryptic specificity allowing up to one miss-cleavage and a tolerance on mass measurement of 10 ppm in MS mode and 20 ppm for MS/MS ions. Structure modifications allowed were oxidized methionine, and deamidation of asparagine and glutamine residues, which were searched as variable modifications. Variable modifications allowed were carbamidomethyl cysteine as a fixed modification. Oxidized methionine, deamidation of Asn and Gln, 13C(6)/15N(2) Lys, and Arg 13C(6)/15N(4) were searched as variable modifications. Using a reversed decoy database, the false discovery rate was less than 1%. Peptide ratios were calculated for each arginine- and/or lysine-containing peptide as the peak intensity of 13C-/15N-labeled arginine/lysine divided by the peak intensity of nonlabeled 12C/14N arginine/lysine for each single-scan mass spectrum. Peptide ratios obtained for each protein were averaged and the standard deviation determined. Only proteins identified with log2 ratios <–0.5 and log2 ratios >0.5 were kept. Only proteins identified with at least two peptides common to the two replicate runs were kept.

Bioinformatic Analyses

For the K/R polybasic motif search, an in lab Linux shell script was used to first download the sequences of the PtdIns(3,4,5)P_3 pulled down proteins from UniProt (curl https://www.uniprot.org/uniprot/) using the curl tool, and search for the (K/R-(X_{3-7})-K-X-K/R-K/R) motif was then carried out using the grep tool.

For the enrichment analyses, the identified UniProt entries were statistically compared with those of the human genome restricted to entries annotated to the nucleus compartment (Gene Ontology [GO]:0050789) using PANTHER classification system version 13.1 (75, 76). The representation for each GO category for biological processes was calculated as the ratio between the cluster (PtdIns(3,4,5)P_3 dataset) frequency and the reference dataset (human nucleome) frequency, the frequency being the percentage of gene entries in a particular GO term category compared with the respective total number of entries. Only enriched categories with p values <0.05 are presented.

The presence of structured PPIn domain was assessed *via* the SMART batch search (http://smart.embl-heidelberg.de/smart/batch.pl).

STRING analysis (77) of all PtdIns(3,4,5)P_3-binding protein entries was based upon experimental prediction methods and a confidence score >0.9.

Immunofluorescence Staining and Microscopy

HeLa cells grown on 12-mm coverslips were fixed with 3.7% (w/v) paraformaldehyde for 10 min and washed twice with PBS. Cells were then permeabilized with 0.25% (v/v) Triton X-100 in PBS for 10 min at RT (to ensure nuclear detection of proteins and lipids at the expense of the integrity of the plasma membrane). Cells were blocked for 1 h with 5% (v/v) goat serum in PBS–0.1% (v/v) Triton X-100. Primary antibody (diluted in the blocking buffer) incubation was performed overnight at 4 °C followed by secondary antibody conjugated to Alexa-488 or Alexa-594 incubation for 1 h at RT. Four washes were performed with PBS containing 0.05% (v/v) Tween-20 (PBS-T), between each antibody incubation. DNA labeling was performed by 15-min incubation with Hoechst 33342. For antibody dilutions, see supplemental Table S2. For cell labeling using the recombinant EGFP-GRP1-PH protein, cells were permeabilized with 0.1% (v/v) Triton X-100 in PBS and blocked in 3% (w/v) fatty acid–free bovine serum albumin and 0.05% (v/v) Triton X-100 in PBS for 1 h at RT. This was followed by incubation with 40 μg/ml of the probe in PBS containing 1% (w/v) fatty acid–free bovine serum albumin and 0.05% (v/v) Triton X-100 for 2 h at RT. Cells were stained with anti-nucleophosmin antibody (1:500) in the same buffer. Images were acquired with a Leica DMI6000B fluorescence microscope using 40× or 100× objectives or Leica TCS SP5 confocal laser scanning microscope using a 63×/1.4 oil-immersion lens. Images were processed with a Leica application suite V 4.0.

SDS-PAGE and Western Immunoblotting

Protein extracts were mixed in 1× Laemmli sample buffer and resolved by SDS-PAGE and then transferred to 0.2-μm nitrocellulose membranes. The membrane was then blocked with 7% (w/v) nonfat milk in PBS-T for 1 h at RT, incubated with anti-GST conjugated to horse radish peroxidase (HRP) antibody for 1 h at RT, or with primary antibodies overnight and secondary antibodies for 1 h at RT. Washes were performed with PBS-T 3 to 4 times after each antibody incubation. The signal was detected by enhanced chemiluminescence using the SuperSignal West Pico Chemiluminescent Substrate (Thermo Fisher) and visualized with a Bio-Rad ChemiDoc Xrs+The enhanced chemiluminescence.

GST-Tagged Recombinant Protein Expression and Purification

The pGEX-4T1-EGFP-GRP1-PH WT and K273A constructs were transformed into *Escherichia coli* BL21-RIL DE3, the bacteria grown at 37 °C and further induced overnight at 18 °C with 0.5 mM IPTG. Bacterial pellets were lysed in 50 mM Tris, pH 7.5, 150 mM NaCl, 10% (v/v) glycerol, 1% (v/v) Triton X-100, 0.5 mg/ml lysozyme, 5 mM DTT, and protease inhibitor cocktail for 30 min on ice. After sonication and centrifugation, GST-EGFP-GRP1-PH was purified with glutathione-agarose 4B beads. Expression and purification of GST-GRP1-PH and GST–phospholipase C δ1 were as described previously (49). The pGEX-6P-2-PARP1 deletion constructs were transformed into *E. coli* BL21-RIL DE3, the bacteria grown at 37 °C and induced for 3 h at 37 °C with 0.5 mM IPTG or overnight at 15 °C (fragment 2 aa 215–371). Bacterial pellets were lysed in 25 mM Tris, pH 8.0, 500 mM NaCl, 0.5% Igepal, and 1× bacterial protease cocktail inhibitor (added fresh) by sonication. Protein purification was performed using glutathione-agarose 4B beads. All protein preparations were analyzed by SDS-PAGE and Coomassie staining.

Lipid Overlay Assay

Lipid overlay assays were performed on hydrophobic membranes, PIP strips (Echelon Biosciences) according to Karlsson *et al.* (25) using anti-PtdIns(3,4,5)P_3 antibody followed by anti-mouse IgG-HRP secondary antibody or 0.5 μg/ml of recombinant proteins (GST (purified as described (25)), GST-PARP1 full length (#80501, BPS Bioscience) or the different PARP1 deletion constructs fused to GST) followed by anti-GST-conjugated to HRP (1:30,000, ab3416, Abcam). Visualization was achieved with enhanced chemiluminescence. Lipid overlay assay of GST-EGFP-GRP1-PH (1.5 μg/ml) was visualized by GFP fluorescence scanning using a Typhoon FLA 9000 scanner with an excitation of 473 nm and a BPB1 filter.

Experimental Design and Statistical Rationale

For the PtdIns(3,4,5)P_3 interactomics, two technical replicates were performed and compared. The first three replicate injections of the same sample (raw files: PR801_CSD_020217_PIP3_SILAC_Inj01/Inj02/Inj03) were processed as a single file (PR801_CSD_020217_PIP3_SILAC_Inj0.msf). The second (raw file PR801_CSD_030217_PIP3_SILAC_3Xinjection) was a technical replicate where three times the amount of peptide as the previous runs was analyzed in a single run. Commonly identified proteins with at least two peptides were kept. The MS proteomics data have been deposited in the ProteomeXchange Consortium *via* the PRIDE partner repository (78) with the dataset identifier PXD020870. Three-four biological replicates were performed for all other experiments, and Student's *t*-tests were used for quantifications.

RESULTS

PtdIns(3,4,5)P_3 *Is Nucleolar in HeLa Cells*

To extend our previous findings on the nucleolar localization of PtdIns(3,4,5)P_3 previously observed in the breast cancer cell line AU565 (25), we determined its subcellular localization in actively growing HeLa cells by immunofluorescence staining and confocal microscopy when permeabilized with Triton X-100 (Fig. 1). Using specific antibodies to detect PtdIns(3,4,5)P_3 ((25) and Fig. 1*B*), we observed the presence of this PPIn in the nucleolus in 74% ± 10% (n = 4) of asynchronous HeLa cells in either intense or diffuse foci that colocalized with the nucleolar proteins nucleolin or upstream binding factor (Fig. 1*D* and supplemental Fig. S1). In addition, the detection of PtdIns(3,4,5)P_3 in the nucleolus was supported using the purified recombinant PH domain of GRP1 (alias cytohesin-3) conjugated to EGFP and GST as a labeling probe. The PH domain of GRP1 is well known for its affinity to PtdIns(3,4,5)P_3, whereas the K273A point mutation disrupts this interaction (79–82). We expressed and purified GST-EGFP-GRP1-PH, which demonstrated interaction with PtdIns(3,4,5)P_3 for the WT but not the K273A mutant when tested by lipid overlay assay (Fig. 1*C*). Fixed asynchronous HeLa cells were labeled with the recombinant WT or K273A probe and immunostained with the nucleolar protein nucleophosmin. When cells were labeled with the WT protein, 51.9% ± 19.1 of the cells showed foci within the rings detected by nucleophosmin (Fig. 1, *E* and *F*). In contrast, the percentage of cells showing these foci was greatly reduced to 3.8% ± 6.7 when using the K273A mutant probe (Fig. 1, *E* and *F*).

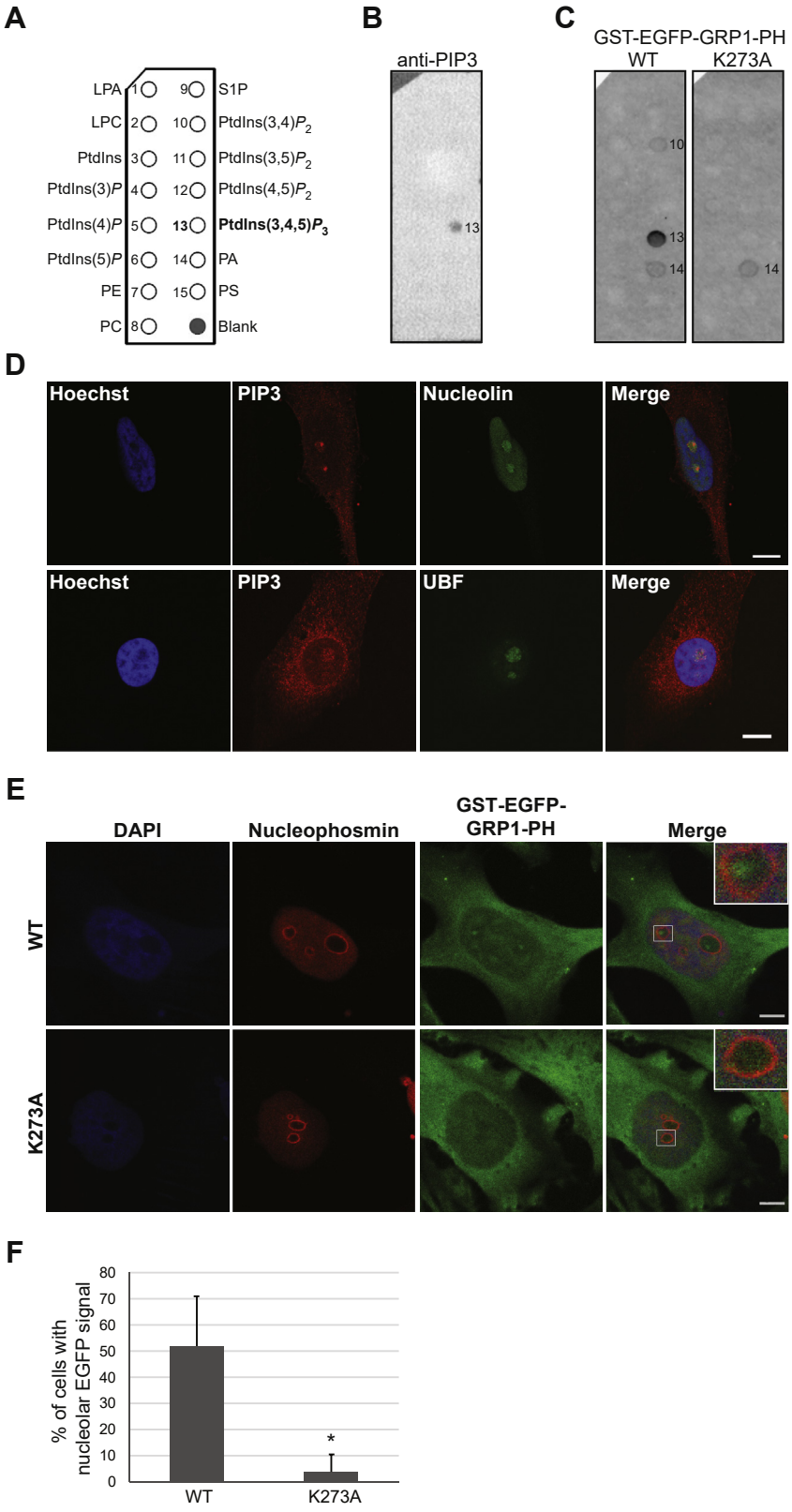

FIG. 1. **Specific detection of PtdIns(3,4,5)P_3 in the nucleolus.** *A*, PIP strip (Echelon Inc) schematic showing the position of the spotted lipids each with 100 pmol. *B*, validation of the anti-PtdIns(3,4,5)P_3 antibody specificity using PIP strips. *C*, validation of the specificity of the recombinant GST-EGFP-GRP1-PH WT *versus* binding mutant K273A. *D* and *E*, confocal microscopy of actively growing HeLa cells stained with

The Nuclear PtdIns(3,4,5)P_3 Interactome Is Enriched in Nucleolar Proteins

The existence of PtdIns(3,4,5)P_3 in the nucleus has been previously reported (19, 24, 25, 66), but so far, only a few nuclear proteins have been reported to interact with PtdIns(3,4,5)P_3 and knowledge of its function is limited in this cell compartment. We sought to identify the interacting partners of PtdIns(3,4,5)P_3 in the nucleus using a quantitative proteomics method previously developed for the identification of nuclear PtdIns(4,5)P_2 effector proteins (49), with a view to identifying nuclear processes that PtdIns(3,4,5)P_3 may regulate. After SILAC labeling of HeLa S3 cells, nuclei were isolated and incubated with neomycin to enrich for and displace potential PPIn-binding proteins from nuclei (Fig. 2*A*). Neomycin is an aminoglycoside that binds to PPIn with high affinity *via* electrostatic interactions (83–85), and we previously showed that it could be used to displace PPIn-binding proteins *via* competitive interaction (49). Equal protein amounts in neomycin-dialysed supernatants, obtained from heavy-labeled and light-labeled cell populations, were incubated with PtdIns(3,4,5)P_3-conjugated beads or control beads, respectively. The specificity of the PtdIns(3,4,5)P_3 affinity beads was validated by a pull-down assay with GST-GRP1-PH (Fig. 2*B*). The control beads showed no affinity, whereas the PtdIns(3,4,5)P_3 beads were able to pull down the GST-GRP1-PH domain. Importantly, this interaction was negligible in the preincubation of free PtdIns(3,4,5)P_3 with the probe. The PtdIns(3,4,5)P_3 and control pull-down eluates were combined and separated by SDS-PAGE. After trypsin digestion, the peptides were analyzed by LC-MS/MS on two replicate runs and identified and quantified using the SEQUEST HT search engine. From these two runs, 179 proteins specifically pulled down by PtdIns(3,4,5)P_3 were commonly identified with at least two peptides (Fig. 2*C* and supplemental Table S3), 75 (42%) of which were identified in two additional experiments (supplemental Table S3). These included proteins previously reported experimentally as *bona fide* nuclear PtdIns(3,4,5)P_3-interacting proteins, that is, nucleophosmin (45), THO complex subunit 4 (47), IQ motif containing GTPase-activating proteins (IQGAP1) (86), as well as OGT (67). In addition to these proteins, 20 from our dataset had previously been identified in PtdIns(3,4,5)P_3 interactomes but characterised from whole-cell extracts (70, 71) (Fig. 2*D* and Table 1). Few proteins were common to the nuclear and whole-cell extract PtdIns(4,5)P_2 interactomes previously reported ((49), Table 2, (71)). Importantly, the majority of the identified proteins are likely to be direct PtdIns(3,4,5)P_3 interactions because only a few clusters involved in protein–protein complexes were detected using the STRING web tool (supplemental Fig. S2). We further searched for the presence of PPIn-binding domains and found only four proteins, including dynamin 1, 2, and 3 harboring a PH domain with previous knowledge of PPIn interaction (87, 88) or ATP binding cassette sub family F member 1 with the less-studied PDZ domain (89). In contrast, the K/R-rich motif (K/R-($X_{n = 3–7}$)-K-X-K/R-K/R), which we previously reported to be enriched in nuclear PtdIns(4,5)P_2-binding proteins (49), was found in 38% of PtdIns(3,4,5)P_3-associated proteins, accounting for a 1.4-fold enrichment compared with proteins pulled down by control beads (Fig. 2*C* and supplemental Table S3) and 1.3-fold compared with proteins annotated to the nucleus (nucleome). For a better understanding of the biological processes of these proteins, they were mapped to the GO database for biological processes and an enrichment test was performed using the PANTHER 14.1 web tool (2019-03-12 release, (75, 76)). The biological processes that were over-represented by >5-fold are shown in Figure 2*E* and listed in supplemental Tables S4, *A–C*. In particular, membrane fission, RNA splicing/processing, protein folding, cytokinesis, and DNA repair were functions particularly enriched in the PtdIns(3,4,5)P_3 pull-down protein list. A large number of the potential PtdIns(3,4,5)P_3 interactors were linked or annotated to the nucleolus, as highlighted in supplemental Table S3. Indeed, 17% of all potential PtdIns(3,4,5)P_3 interactors are common to the nucleolar database (90) and 51% to the T cell nucleome (72), including 19 common to both nucleome lists.

PtdIns(3,4,5)P_3 Interacts With PARP1 and Both Localize in Nucleoli

PARP1 is a chromatin-associated protein that has also been reported to be abundant in the nucleolus (91–93). In this study, PARP1 was identified as a PtdIns(3,4,5)P_3-interacting protein with a PtdIns(3,4,5)P_3/control SILAC ratio of 2.5 (Table 1 and supplemental Table S3). We first validated the effect of neomycin on displacing PARP1 as well as other PtdIns(3,4,5)P_3-binding proteins from the nuclear environment to the supernatant by Western immunoblot analyses (Fig. 3*A*). We then biochemically validated the direct interaction of the full-length PARP1 with PPIn by lipid overlay assay using phospholipid-immobilized strips and GST-PARP1 recombinant protein

the indicated antibodies (*D*) or by incubation with recombinant GST-EGFP-GRP1-PH WT or K273A mutant combined with anti-nucleophosmin staining (*E*). *F*, quantification of the detection of nucleolar PtdIns(3,4,5)P_3 expressed as the percentage of HeLa cells showing foci detected by the GST-EGFP-GRP1-PH probe WT or K273A mutant within the area delimited by nucleophosmin (mean + SDs, $n = 3$, $^*p < 0.05$ two-way unpaired Student's *t* test). The scale bar represents 5 μm. GRP1, general receptor for phosphoinositides-1; LPA, lysophosphatidic acid; LPC, lysophosphatidylcholine; PA, phosphatidic acid; PC, phosphatidylcholine; PE, phosphatidylethanolamine; PH, pleckstrin homology; PI, phosphatidylinositol; PIP3, PtdIns(3,4,5)P_3; PS, phosphatidylserine; PtdIns(3,4,5)P_3, phosphatidylinositol 3,4,5-trisphosphate; S1P, sphingosine-1-phosphate; UBF, upstream binding factor.

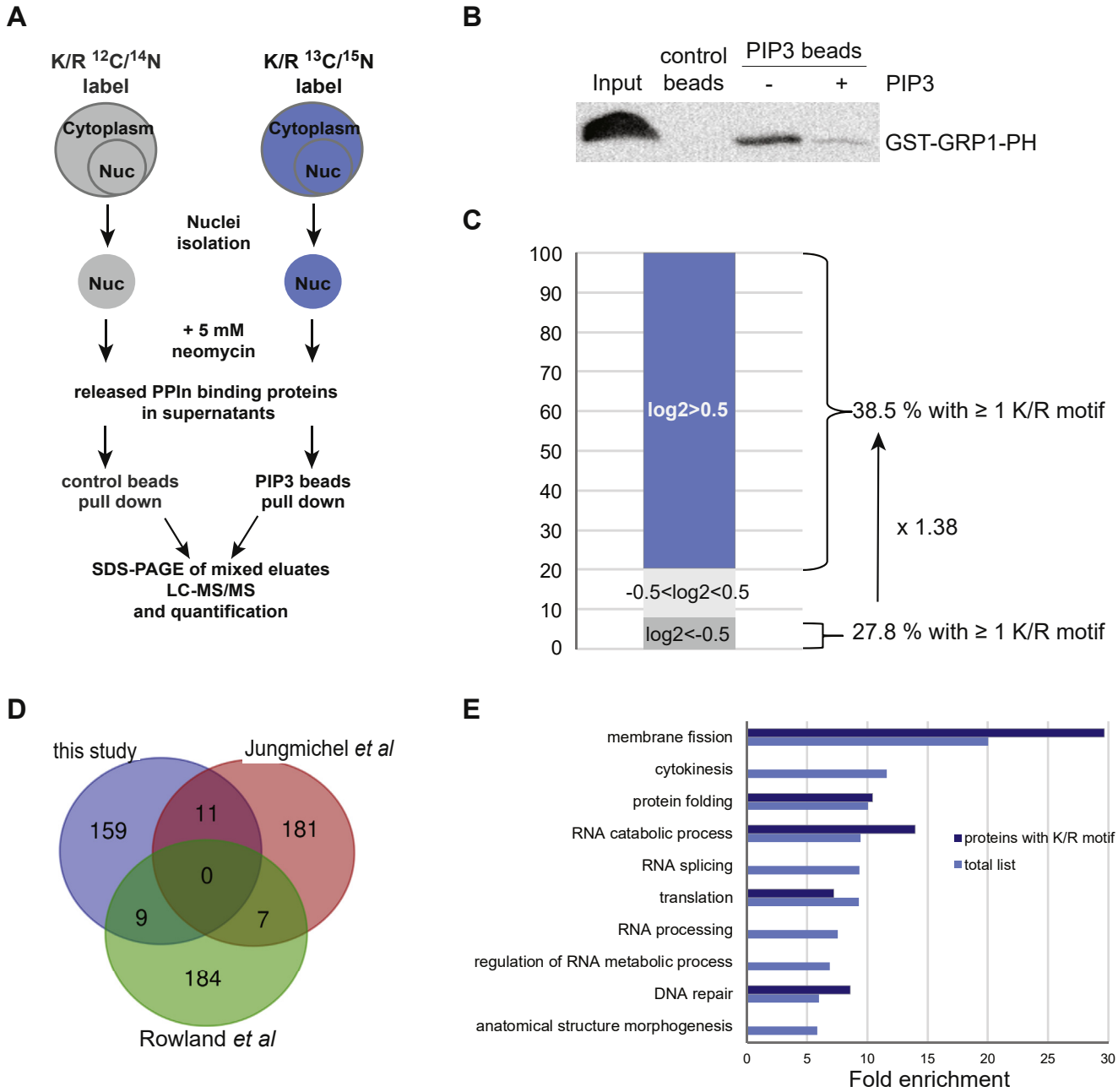

FIG. 2. **Nuclear PtdIns(3,4,5)P_3 interactome.** *A*, the workflow of the experimental setup where heavy-labeled and unlabeled HeLa S3 nuclei were incubated with 5 mM neomycin and the displaced proteins pulled down using control beads or PIP3-conjugated beads, resolved by SDS-PAGE through the stacking gel and subsequently analyzed by LC-MS/MS. *B*, GST-GRP1-PH pull down with control or PIP3-conjugated beads in the absence (-) or presence (+) of 20 μM free PIP3. Eluates were resolved by SDS-PAGE and Western blotted using an anti-GST antibody conjugated to horse radish peroxidase. *C*, protein distribution in percentage according to their log2 values: proteins with log2 <–0.5 (binding to control beads, 18 proteins), –0.5 < log2 < 0.5 (proteins binding equally to PIP3 or control beads, 26 proteins), and log2 >0.5 (binding to PIP3 beads, 179 proteins). *D*, the Venn diagram comparing the PIP3 interactome from this study with two others (70, 71). *E*, biological processes of Gene Ontology fold enrichment of the proteins pulled down specifically by the PIP3-conjugated beads from this study with an FDR $p < 0.05$ and with at least five proteins in each process. See proteins listed in supplemental Tables S4, *A–C*. FDR, false discovery rate; PH, pleckstrin homology; PIP3, phosphatidylinositol 3,4,5-trisphosphate.

(Fig. 3*B*). PARP1 was found to interact with most PPIns as well as other anionic glycerophospholipids, phosphatidic acid (PA) and phosphatidylserine, but not with other glycerophospholipids or sphingosine 1-phosphate. In contrast, GST alone showed no interaction. We validated these results using a PPIn pull-down assay and demonstrated

TABLE 1
List of PtdIns(3,4,5)P_3-binding proteins common to two other reported PtdIns(3,4,5)P_3 interactomes

UniProt ID	Protein name description	Gene name	MW (kDa)	SILAC ratio	K/R motif
P29372	DNA-3-methyladenine glycosylase	MPG	33	18.812	-
Q9UPQ0	LIM and calponin homology domains-containing protein 1	LIMCH1	122	9.439	+
Q13112	Chromatin assembly factor 1 subunit B	CHAF1B	61	3.057	-
P09874	Poly [ADP-ribose] polymerase 1	PARP1	113	2.5	+
Q52LJ0	Protein FAM98B	FAM98B	37	2.408	-
P78347	General transcription factor II-I	GTF2I	112	2.236	-
Q16531	DNA damage-binding protein 1	DDB1	127	2.101	-
P62136	Serine/threonine-protein phosphatase PP1-alpha catalytic subunit	PPP1CA	37	1.939	+
Q05682	Caldesmon	CALD1	93	1.705	+
P33992	DNA replication licensing factor MCM5	MCM5	82	1.538	-
P35579	Myosin-9	MYH9	226	5.071	+
P26599	Polypyrimidine tract-binding protein 1	PTBP1	57	2.991	+
P53396	ATP-citrate synthase	ACLY	121	2.985	-
P13010	X-ray repair cross-complementing protein 5	XRCC5	83	2.817	-
P12814	Alpha-actinin-1	ACTN1	103	2.56	+
O43707	Alpha-actinin-4	ACTN4	105	2.366	+
P62826	GTP-binding nuclear protein Ran	RAN	24	2.205	+
P49736	DNA replication licensing factor MCM2	MCM2	102	1.68	-
P60228	Eukaryotic translation initiation factor 3 subunit E	EIF3E	52	1.599	-
P51610	Host cell factor 1	HCFC1	209	1.626	-

Proteins pulled down by PtdIns(3,4,5)P_3 identified in this study common to those in PtdIns(3,4,5)P_3 interactome lists from Jungmichel *et al.* (71), indicated in light gray, Rowland *et al.* (70) in white, and Bidlingmaier *et al.* (50) in dark gray.

narrower specificity of interaction of GST-PARP1 to PtdIns(3,4)P_2 and PtdIns(3,4,5)P_3 and lack of interaction to PtdIns(4,5)P_2 or the monophosphorylated PPIn (Fig. 3*C*, left panel). To control for the lack of interaction with PtdIns(4,5)P_2, we tested the PtdIns(4,5)P_2-conjugated beads with the PH domain of phospholipase Cδ1 and showed a strong interaction (Fig. 3*C*, right panel). The nuclear presence of PtdIns(4,5)P_2 and PtdIns(3,4,5)P_3 is well established, and we compared the endogenous localization of these lipids to PARP1 by immunofluorescence staining. PtdIns(3,4,5)P_3 and PARP1 colocalized in the nucleolus in 21.5 ± 6.9% of HeLa cells (n = 4) (Fig. 3*D* and supplemental Fig. S3). In contrast, PtdIns(4,5)P_2 segregated to nuclear speckles, consistently to previous studies (20, 21), and mostly did not colocalize with PARP1 (Fig. 3*D* and supplemental Fig. S4). Considering the interaction of PARP1 with PtdIns(3,4)P_2 in the pull-down assay, we determined their localization and showed that nucleoplasmic PARP1 tended to localize in PtdIns(3,4)P_2-positive foci in some cells (Fig. 3*D* and supplemental Fig. S5). In sum, PARP1 was shown to interact with several PPIns *in vitro* but commonly localizes at sites of the nucleus showing a strong presence for PtdIns(3,4)P_2 and PtdIns(3,4,5)P_3.

TABLE 2
List of PtdIns(3,4,5)P_3-binding proteins common to the nuclear PtdIns(4,5)P_2 interactome

UniProt ID	Protein name description	Gene name	MW (kDa)	SILAC ratio	
				PIP3 list	PIP2 list
P11021	78-kDa glucose-regulated protein	HSPA5	72	1.787	1.63
Q9P258	Protein RCC2	RCC2	56	2.305	1.869
P26599	**Polypyrimidine tract-binding protein 1**	**PTBP1**	57	**2.991**	**1.964**
O60506	**Heterogeneous nuclear ribonucleoprotein Q**	**SYNCRIP**	69	**1.504**	**2.033**
P68104	Elongation factor 1-alpha 1	EEF1A1	50	2.007	2.072
Q99729	**Heterogeneous nuclear ribonucleoprotein A/B**	**HNRNPAB**	36	**2.604**	**2.272**
Q14103	**Heterogeneous nuclear ribonucleoprotein D**	**HNRNPD**	38	**2.345**	**2.44**
P23284	Peptidyl-prolyl *cis-trans* isomerase B	PPIB	24	2.342	2.450
Q00839	**Heterogeneous nuclear ribonucleoprotein U**	**HNRNPU**	90	**1.742**	**2.676**
P26641	Elongation factor 1-gamma	EEF1G	50	1.565	2.84
P29692	Elongation factor 1-delta	EEF1D	31	2.078	2.89

Proteins pulled down by PtdIns(3,4,5)P_3 (PIP3) identified in this study common to those reported in the PtdIns(4,5)P_2 (PIP2) nuclear interactome that we have previously published (49). Proteins highlighted in bold indicate proteins with roles in splicing.

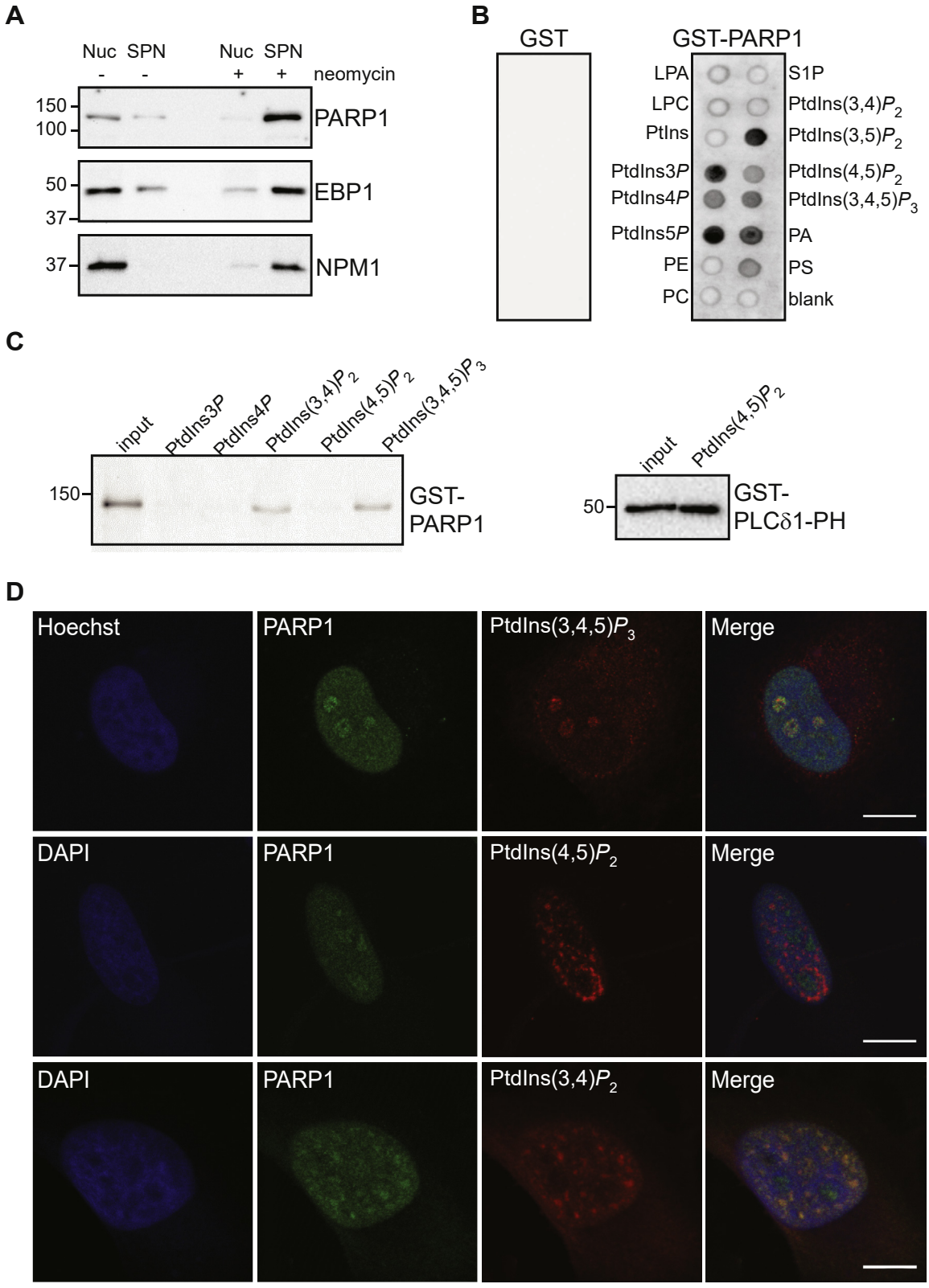

FIG. 3. **PtdIns(3,4,5)P_3 interacts and colocalizes with PARP1 in the nucleolus.** *A*, Western immunoblotting of supernatants (SPN) and resulting nuclear pellets (NUC) obtained after the incubation of isolated HeLa nuclei in the retention buffer in the absence (-) or presence (+) of neomycin. *B*, lipid overlay assay using PIP strips incubated with recombinant GST or GST-PARP1 and detection of protein–lipid interactions using an anti-GST-HRP–conjugated antibody. *C*, GST-PARP1 or GST-PLCδ1-PH pulldown with the indicated PPIn-conjugated beads. Eluates

PARP1 Binds to PPIn via PBRs Located in the Zinc Finger III and the BRCT–WGR Linker

PARP-1 is organized in several structural and functional domains including the N-terminal DNA-binding domain consisting of three zinc fingers (ZnFs), an automodification domain, a Trp-Gly-Arg (WGR) domain, and a C-terminal catalytic region consisting of the helical and (ADP-ribosyl) transferase domains (Fig. 4*A*). We first systematically tested the ability of the different PARP1 regions to bind to PPIns *via* a lipid overlay assay and found that three regions contributed to the interaction, including the ZnF-I, ZnF-III, and the linker located between the BRCA1 C terminus (BRCT) and WGR domains (Fig. 4, *B* and *C*). These regions also showed strong interaction with PA. After a closer investigation of the amino sequence of these regions, four PBRs were found, including a K/R motif in the ZnF-I (78-RWDDQQKVKK-87), two in the ZnF-III (221-KKKSKKEKDKDSKLEK-236 and 346-KKLKVKK-352), and a reverse K/R motif (505-KKSKGQVK-512) located in the linker between the BRCT and WGR domains. To test whether these PBRs were responsible for the interaction of PARP1 with PPIn, we generated four mutants by either mutating lysine residues to alanines or leucines in the ZnF-I (^{84}KVKK^{87}) and the linker (^{505}KKSK^{508}) or deleting the whole PBR containing more than three lysines in the ZnF-III. Using lipid overlay assays, the triple mutant located in the ZnF-I (^{84}AVLL^{87}) did not show any change in overall binding compared to the WT (Fig. 4*D*). In contrast, the other three PBR mutants, the ZnF-III Δ221 to 36, Δ346 to 52, or linker triple mutant (^{505}AASL^{508}) showed a great reduction in binding to PPIn and PA (Fig. 4*D*). The PBRs located in the ZnF-III are well conserved in vertebrates and are accessible to solution as shown in the NMR structure as red highlights (Fig. 4, *E* and *F*), suggesting an important role for these sites. The linker PBR is only conserved in mammals (Fig. 4*E*).

DISCUSSION

Evidence of the presence of PPIn in the nucleus together with the kinases responsible for their synthesis is now well established (37, 41, 94–96). Interestingly, they are found in RNA-rich membrane-less compartments, such as the nuclear speckles and nucleolus in particular for PtdIns(4,5)P_2 (20–22, 56) and PtdIns(3,4,5)P_3 (25), respectively. In this study, we have extended our previous findings (25) by showing the localization of PtdIns(3,4,5)P_3 in the nucleolus in HeLa cells. To support these findings, a minor pool of PtdIns(4,5)P_2 has been previously reported in the nucleolus and could hence substantiate the nucleolar synthesis of PtdIns(3,4,5)P_3 (21, 62). In addition, the PPIn kinase isoforms, PI4K IIα, PIP5K Iα, and PI3K p110β which synthesize PtdIns4*P*, PtdIns(4,5)P_2, and PtdIns(3,4,5)P_3 respectively, have all been shown to be present in the nucleolus (25, 28, 97, 98). Similarly, some evidence point to the presence of the PtdIns(3,4,5)P_3 phosphatases, phosphatase and tensin homolog and Src homology 2 domain–containing inositol phosphatase (SHIP) in the nucleolus (99, 100). All the components are therefore in place in nucleoli for the regulation of PtdIns(3,4,5)P_3 synthesis and a potential role in this subnuclear compartment. The biophysico-chemical form in which PtdIns(3,4,5)P_3 exists in a nonmembranous environment such as the nucleolus is unclear. How the acyl chains can be sheltered from the aqueous environment may be explained by the formation of micelles from the aggregation of acyl chains (94, 101), but this has not been demonstrated so far. Aggregates of PtdIns(4,5)P_2 in nuclear lipid islets in the nucleoplasm have recently been described and consist of proteo-lipid aggregates of about 100 nm in size (34). The PtdIns(3,4,5)P_3 foci detected *via* confocal microscopy may indicate the presence of PtdIns(3,4,5)P_3 nucleolar aggregates. This would imply that the acyl chains of PtdIns(3,4,5)P_3 are shielded from the nuclear environment within the core of micelle-like foci, giving a plausible explanation for the biophysical presence of such lipids in the absence of membranes. This remains however to be further explored.

To further decipher the role(s) of nuclear PtdIns(3,4,5)P_3, we applied the quantitative interactomics method that we had previously developed (49). To this end, we have identified 179 proteins specifically pulled down by PtdIns(3,4,5)P_3 and not by control beads. Our study allowed the identification of nuclear effector proteins, the majority of which were not identified in the previous interactome performed from whole-cell extracts (71). The highest proportion of PtdIns(3,4,5)P_3 interactors were indeed annotated to other compartments than the nucleus in that study, hence masking potential nuclear effector proteins. Except for a few proteins known to be engaged in protein–protein complexes, the remaining proteins identified in this study are likely to be direct PtdIns(3,4,5)P_3 interactors. Several of the identified proteins in this study have previous history as nuclear PPIn effector proteins, such as nucleophosmin, OGT, IQGAP1, and THO complex 4 and have well-characterized PPIn-binding sites (45, 47, 67, 86). When searching for the presence of PPIn domains, only three proteins identified in this study have structured PPIn-interacting domains, that is, dynamin 1 to 3, each harboring a PH domain (87, 88). The PH domain of these proteins has been reported to bind to PtdIns(4,5)P_2 (87, 88) but also to PtdIns(3,4,5)P_3 in another

were resolved by SDS-PAGE and Western blotted using an anti-GST antibody conjugated to horse radish peroxidase. *D*, HeLa cells costained with anti-PARP1 and anti-PtdIns(3,4,5)P_3, anti-PtdIns(4,5)P_2, or anti-PtdIns(3,4)P_2 antibodies and imaged by confocal microscopy. The scale bar represents 10 μm. Images are representative of at least three biological replicates. PPIn, polyphosphoinositide; PtdIns(3,4)P_2, phosphatidylinositol 3,4-bisphosphate; PtdIns(3,4,5)P_3, phosphatidylinositol 3,4,5-trisphosphate; PARP1, poly(ADP-ribose) polymerase 1; PtdIns(4,5)P_2, phosphatidylinositol 4,5-bisphosphate.

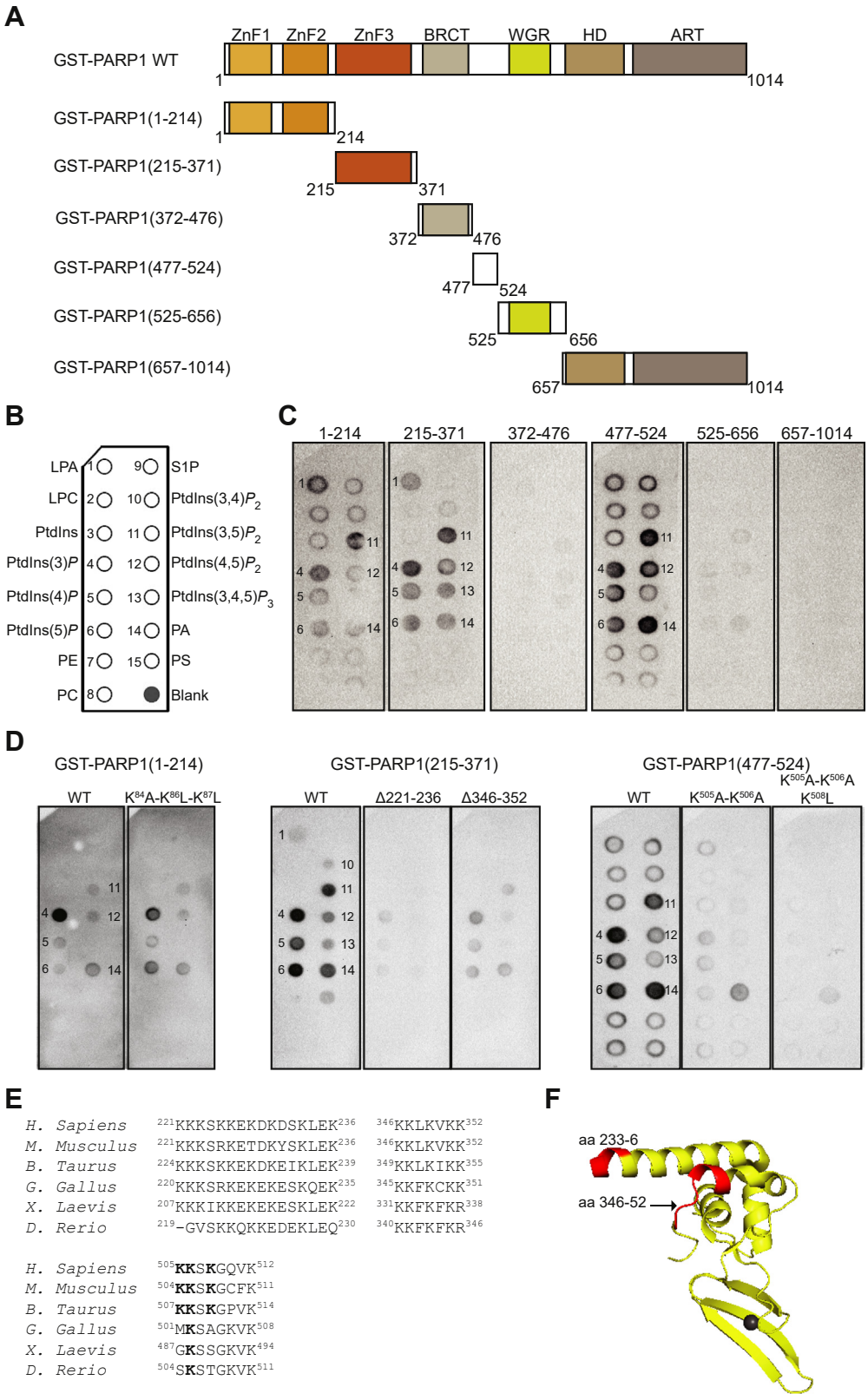

FIG. 4. **PARP1 binds to PPIn *via* three polybasic regions.** *A*, domain structure of PARP1 and deletion constructs. *B*, schematic representation of lipids spotted (100 pmol) on PIP strips (Echelon Biosciences) including lysophosphatidic acid (LPA), lysophosphatidylcholine (LPC), phosphatidylinositol (PtdIns), PtdIns3*P*, PtdIns4*P*, PtdIns5*P*, phosphatidylethanolamine (PE), phosphatidylcholine (PC), sphingosine-1-

TABLE 3
List of potential PtdIns(3,4,5)P_3-binding proteins annotated to DNA repair

UniProt ID	Name description	Gene name	SILAC ratio	K/R motif	Study		
					1	2	3
P29372	DNA-3-methyladenine glycosylase	MPG	18.81	-	+	-	-
P13010	X-ray repair cross-complementing protein 5	XRCC5	2.817	-	-	+	-
P09874	Poly [ADP-ribose] polymerase 1	PARP1	2.5	RWDDQQKVKK	+	+	-
P46063	ATP-dependent DNA helicase Q1	RECQL	2.271	KNTGAKKRK	-	+	-
P12956	X-ray repair cross-complementing protein 6		2.215	-	+	+	-
P78527	DNA-dependent protein kinase catalytic subunit	PRKDC	2.112	KHVSLNKAKKRR	-	+	-
P49916	DNA ligase 3	LIG3	2.119	KRHWLKVKK	-	+	-
Q92466	DNA damage-binding protein 2	DDB2	2.474	-	-	-	-
O60934	Nibrin	NBN	1.575	KNFKKFKK RYNPYLKRRR KEEEEEEKPKR KKEEIKDEKIKK	-	-	-

Proteins pulled down by PtdIns(3,4,5)P_3 and annotated to the DNA repair–enriched process, identified with at least two peptides, with heavy/light log2 ratios >0.5, are indicated in this table. Their presence (highlighted +) or absence (–) in the nucleolar database (study 1, (90)), the T cell nucleome (study 2, (72)), and/or the HeLa nucleome (study 3, (103)) is indicated. K/R motifs consist of the following sequence: K/R-($X_{n = 3–7}$)-K-X-K/R-K/R.

study (102). Although dynamin family members are GTPase considered to be localized on membranes and microtubules, dynamin 2 and 3 were also identified in nucleolar proteomes (72, 103). The function of dynamin in the nucleolus has however not been investigated so far. IQGAP1 binds to PtdIns(3,4,5)P_3 *via* an atypical PPIn-binding domain lined with basic residues, with a distinct fold to most known domains (86). Although IQGAP1 has clear roles in the cytoplasm, it was also reported to accumulate in the nucleus at the G1/S phase of the cell cycle (104). Still how PPIn binding affects its nuclear role is unknown.

The majority of the PtdIns(3,4,5)P_3 interactors identified in this study are characterized by the presence of at least one K/R motif. These motifs have been previously shown to be enriched in the nuclear PtdIns(4,5)P_2 interactome (49) and to serve as a PPIn interaction site in other nuclear proteins *via* electrostatic interactions between basic residues and the phosphate groups on the inositol ring (25, 44, 46, 48, 51–55). The reported nuclear PPIn-binding proteins tend not to show distinct affinity *in vitro* and can bind to monophosphorylated PPIn, diphosphorylated PPIn, or PtdIns(3,4,5)P_3. This would suggest that these motifs may not provide specific interaction between the different PPIns *per se*. This appears to be inherent to such PBR also in membrane-targeted proteins (105, 106). Specific interaction may be due *in vivo* to the local availability of PPIn pools generated by specific PPIn kinases or phosphatases near PPIn-binding proteins. In addition, protein interactions may contribute to the local specificity of interaction. For example, the previously reported interaction of PARP1 with nucleophosmin (92), which also binds PtdIns(3,4,5)P_3 (45), may bring PARP1 in close proximity to PtdIns(3,4,5)P_3 in the nucleolus.

In this study, we have shown that the full-length PARP1 binds directly to PPIn *in vitro* using lipid overlay assay and PPIn pulldown. The pull-down assay showed some interaction specificity toward PtdIns(3,4,5)P_3 and PtdIns(3,4)P_2 compared with the lipid overlay assay showing little specificity for the different PPIn species. Lipid presentation is different in these two assays and include the glycerol backbone as well as short acyl chains composed of six carbons when the PPIn-conjugated beads are used. This may explain the difference in specificity and may suggest that hydrophobic interactions contribute to the specificity of interaction. Consistent with the idea that specificity of interaction may be due to the presence of subnuclear pools of different PPIns, PARP1 colocalized with PtdIns(3,4,5)P_3 in the nucleolus and with PtdIns(3,4)P_2 in nucleoplasmic foci, and not with PtdIns(4,5)P_2. The localization of PtdIns(3,4)P_2 in nucleoplasmic foci is consistent with

Phosphate (S1P), PtdIns(3,4)P_2, PtdIns(3,5)P_2, PtdIns(4,5)P_2, PtdIns(3,4,5)P_3, phosphatic acid (PA), phosphatidylserine (PS), and blank. *C* and *D*, lipid overlay assay using PIP strips incubated with recombinant GST-PARP1 deletion constructs WT and mutants and detection of protein–lipid interactions using an anti-GST-HRP–conjugated antibody. *E*, multiple sequence alignment of the polybasic regions located in the zinc finger III and the BRCT-WGR linker found in human PARP-1 compared with other vertebrate species performed using the online program MUSCLE. Accession number for *Homo sapiens* (P09874), *Mus musculus* (P11103), *Bos taurus* (P18493), *Gallus gallus* (P26446), *Xenopus laevis* (P31669), and *Danio rerio* (Q5RHR0). *F*, *ribbon* representation of the human PARP-1 zinc-finger III NMR structure (aa 233–357 PDB: 2JVN, (126)). The two polybasic regions found in the N-terminal (aa 233–236) and C-terminal (aa 346–352) parts of the zinc-finger III are colored in *red*. ART, (ADP-ribosyl) transferase domain (ART); BRCT, BRCA1 C-terminal domain; HD, helical subdomain; HRP, horse radish peroxidase; PARP1, poly(ADP-ribose) polymerase 1; ZnF 1 to 3, zinc-finger I-III; WGR, Trp-Gly-Arg.

recent studies (13, 27). The identity of these foci has not been investigated but appear to be distinct to PtdIns(4,5)P_2-positive sites that localize to nuclear speckles (21) but not with PARP1. Knowledge of the synthesis route of PtdIns(3,4)P_2 in the nucleus is limited but was shown in one study to be produced by the 5-phosphatase, SHIP2, by dephosphorylating PtdIns(3,4,5)P_3 in vascular smooth muscle cells (107). SHIP2 (107) or in its phosphorylated form on serine 132 (108) was found in nuclear speckles in different cells. Alternatively, the class II PI3K, PI3KC2α, known to produce PtdIns(3,4)P_2 by phosphorylating PtdIns4*P*, was also reported to localize in nuclear foci (109) as well as its substrate PtdIns4*P* (26, 27), thus suggesting a potential synthesis route for PtdIns(3,4)P_2 in nuclear speckles. A key question is whether PtdIns(3,4)P_2 and PtdIns(3,4,5)P_3 bind to or even recruit PARP1 to their nuclear sites.

Using deletion constructs determined that the interaction was restricted to the ZnF-I, ZnF-III, and a linker region between the BRCT and the WGR domains but with different specificity. PARP1 does not harbor any known folded PPIn-binding domain but binds to PPIn *via* three PBRs located in the ZnF-III and the linker composed of lysine clusters. Deletion of the clusters in the ZnF-III or mutation of lysines to neutral residues in the linker greatly diminished the interaction with PPIn. The ZnF-I showed interaction with PPIn and PA with some specificity toward PtdIns3*P*, but it is however unclear how the ZnF-I interacts with PPIn. The lysine clusters shown to contribute to PARP1-PPIn interaction are consistent to sites of interaction identified in other nuclear proteins including EBP1 (25), PHD factor 1 (46), PHD finger protein 8 (110), sin3A-associated protein 30-like (111), brain acid soluble protein 1 (51), transcription initiation factor TFIID subunit 3 (53), and BROMO domain adjacent to zinc finger 2B (54). In contrast to all these examples, but except for EBP1, PARP1 interacts with PPIn *via* several PBRs, and it is not yet clear how they each contribute individually and if they provide different affinities for PtdIns(3,4)P_2 or PtdIns(3,4,5)P_3 in the nucleus.

The nucleolar protein, nucleophosmin, has previously been shown to bind the DNA-binding domain of PARP-1 (92), and it is in addition a well-known PtdIns(3,4,5)P_3-interacting protein (45). When cells are not under stress conditions, an enrichment of both PARP1 and poly ADP-ribose can be observed in the nucleolus (92, 112). Upon RNA polymerase I inhibition, PARP1 delocalizes from the nucleolus, indicating that the presence of PARP1 in the nucleolus is dynamic and dependent on RNA polymerase I transcriptional activity. Nucleolar delocalization of PARP1 is accompanied by other nucleolar proteins such as nucleophosmin and upstream binding factor (92, 113, 114). Altogether, these studies suggest that the integrity of the organization of proteins within the nucleolus is dependent upon the active transcription of rRNA. Considering that PARP1 was reported to interact with nucleophosmin *via* its DNA-binding domain (92), which also interacts with PPIn, a complex formed between PARP1, nucleophosmin and PtdIns(3,4,5)P_3 could exist in the nucleolus, but its role is still unclear.

The PtdIns(3,4,5)P_3-binding protein list was highly enriched in nucleolar proteins. The nucleolus is a compartment where rRNA transcription and processing occur to enable ribosome subunit biogenesis (115). However, GO analyses of nucleolar proteomes showed their association with other biological functions such as cell cycle regulation and DNA repair (115, 116). Indeed, a growing body of evidence indicates that some nucleolar proteins have roles in DNA repair (116–119). Interestingly, among the PtdIns(3,4,5)P_3-interacting proteins identified in this study, an enrichment of DNA repair proteins was shown, listing nine proteins, seven of which were found in at least one of the nucleome datasets previously published, including PARP1 ((72), see also Table 3). This could be consistent with the link between PtdIns(3,4,5)P_3 and DNA repair shown in previous studies (66, 120). In particular, PtdIns(3,4,5)P_3 was shown to accumulate at damaged DNA sites upon UV irradiation (120). Protein folding/response to heat was also an enriched biological function in the PtdIns(3,4,5)P_3-interacting protein dataset, which contained several molecular chaperones and heat-shock proteins (HSPs) 70/90. Although their localization and roles are dominantly described in the cytoplasm, several of them are also found in the nucleus, including HSPA1B, HSPA2, HSPA8, HSPA9, as well as HSP90 (121, 122) but also in the nucleolus (HSPA1, (123, 124)). A link between the nucleolus and HSPA1-mediated protein quality control has been recently demonstrated (124). Some HSPs have reported roles in DNA repair (125) and of particular interest here is the interaction shown between HSPA1 and PARP1 and the importance of HSPA1 in DNA breaks protection (123). Again, how nuclear PPIns including PtdIns(3,4,5)P_3 come into play remains to be explored.

In conclusion, this study extends our knowledge of PtdIns(3,4,5)P_3-interacting proteins already identified from cytoplasmic or whole-cell extract sources and further acknowledges the complexity of these interactions in the nucleus. Our approach based on neomycin-dependent displacement of proteins allowed the identification of numerous nuclear PtdIns(3,4,5)P_3 partners, with perhaps noncanonical nucleolar roles. This resource is amenable for further biochemical and functional characterization assessing the array of nuclear, and in particular nucleolar, functions these interactions can regulate.

DATA AVAILABILITY

The raw mass spectrometry data are available on the ProteomeXchange Consortium *via* the PRIDE partner repository (PXD020870).

Supplemental data—This article contains supplemental data.

Acknowledgments—We would like to thank Dr Bernd Thiede (University of Oslo, Norway) for validating the efficiency of the incorporation of heavy amino acids for SILAC. We thank Dr Julien Viaud (INSERM U1048 and Université Toulouse III, France) for the pGEX-4T1-EGFP-GRP1-PH construct. We thank Dr Olena Dobrovolska for the initial identification of residues important for the interaction of PARP1 fragment 4 with PPIn by NMR and Timothée Chaillet for his enthusiasm and work on the PARP1 constructs 3 and 4. This project was funded by the University of Bergen, the Nansen Fond, and the Meltzer Foundation.

Author contributions—F. M. G., M. S. S., A. P. M., V. S. A., S. N., C. S. D., and A. E. L. investigation; F. M. G. and A. E. L. visualization; F. M. G. and A. E. L. writing–original draft; M. S. S., A. P. M., D. C. T., S. N., C. S. D., and A. E. L. writing–reviewing and editing; D. C. T. and A. E. L. supervision; S. N. validation; C. S. D. and A. E. L. methodology; C. S. D. and A. E. L. formal analysis; A. E. L. conceptualization; A. E. L. project administration; A. E. L. funding acquisition.

Conflict of interest—The authors declare no competing interests.

Abbreviations—The abbreviations used are: BRCT, BRCA1 C terminus; EBP1, ErbB3-binding protein 1; GO, gene ontology; GRP1, general receptor of phosphoinositides-1; HRP, horse radish peroxidase; HSPs, heat-shock proteins; IQGAP1, IQ motif containing GTPase-activating proteins; OGT, O-linked N-acetylglucosamine transferase 110-kDa subunit; PA, phosphatidic acid; PARP1, poly(ADP-ribose) polymerase 1; PBRs, polybasic regions; PBS-T, PBS containing 0.05% Tween-20; PH, pleckstrin homology; PI3K, phosphoinositide 3-kinase; PPIn, polyphosphoinositide; PtdIns, phosphatidylinositols; PtdIns(3,4)P_2, phosphatidylinositol 3,4-bisphosphate; PtdIns(3,4,5)P_3, phosphatidylinositol 3,4,5-trisphosphate; PtdIns(4,5)P_2, phosphatidylinositol 4,5-bisphosphate; PtdIns4*P*, phosphatidylinositol 4-phosphate; SHIP, Src homology 2 domain–containing inositol phosphatase; SILAC, stable isotope labeling with amino acids in cell culture; WGR, Trp-Gly-Arg domain; ZnF, zinc finger.

Received March 22, 2021 Published, MCPRO Papers in Press, xxx, https://doi.org/10.1016/j.mcpro.2021.100102

REFERENCES

1. Michell, R. H., Heath, V. L., Lemmon, M. A., and Dove, S. K. (2006) Phosphatidylinositol 3,5-bisphosphate: Metabolism and cellular functions. *Trends Biochem. Sci.* **31**, 52–63
2. Dickson, E. J., and Hille, B. (2019) Understanding phosphoinositides: Rare, dynamic, and essential membrane phospholipids. *Biochem. J.* **476**, 1–23
3. Maffucci, T. (2012) An introduction to phosphoinositides. *Curr. Top. Microbiol. Immunol.* **362**, 1–42
4. Sasaki, T., Takasuga, S., Sasaki, J., Kofuji, S., Eguchi, S., Yamazaki, M., and Suzuki, A. (2009) Mammalian phosphoinositide kinases and phosphatases. *Prog. Lipid Res.* **48**, 307–343
5. Schink, K. O., Tan, K. W., and Stenmark, H. (2016) Phosphoinositides in control of membrane dynamics. *Annu. Rev. Cell Dev. Biol.* **32**, 143–171
6. Fiume, R., Faenza, I., Sheth, B., Poli, A., Vidalle, M. C., Mazzetti, C., Abdul, S. H., Campagnoli, F., Fabbrini, M., Kimber, S. T., Mariani, G. A., Xian, J., Marvi, M. V., Mongiorgi, S., Shah, Z., *et al*. (2019) Nuclear phosphoinositides: Their regulation and roles in nuclear functions. *Int. J. Mol. Sci.* **20**, 2991
7. Jacobsen, R. G., Mazloumi Gavgani, F., Edson, A. J., Goris, M., Altankhuyag, A., and Lewis, A. E. (2019) Polyphosphoinositides in the nucleus: Roadmap of their effectors and mechanisms of interaction. *Adv. Biol. Regul.* **72**, 7–21
8. Cocco, L., Gilmour, R. S., Ognibene, A., Letcher, A. J., Manzoli, F. A., and Irvine, R. F. (1987) Synthesis of polyphosphoinositides in nuclei of Friend cells. Evidence for polyphosphoinositide metabolism inside the nucleus which changes with cell differentiation. *Biochem. J.* **248**, 765–770
9. Payrastre, B., Nievers, M., Boonstra, J., Breton, M., Verkleij, A. J., and Van Bergen en Henegouwen, P. M. (1992) A differential location of phosphoinositide kinases, diacylglycerol kinase, and phospholipase C in the nuclear matrix. *J. Biol. Chem.* **267**, 5078–5084
10. Cocco, L., Martelli, A. M., Gilmour, R. S., Ognibene, A., Manzoli, F. A., and Irvine, R. F. (1988) Rapid changes in phospholipid metabolism in the nuclei of Swiss 3T3 cells induced by treatment of the cells with insulin-like growth factor I. *Biochem. Biophys. Res. Commun.* **154**, 1266–1272
11. Divecha, N., Banfic, H., and Irvine, R. F. (1991) The polyphosphoinositide cycle exists in the nuclei of Swiss 3T3 cells under the control of a receptor (for IGF-I) in the plasma membrane, and stimulation of the cycle increases nuclear diacylglycerol and apparently induces translocation of protein kinase C to the nucleus. *EMBO J.* **10**, 3207–3214
12. Martelli, A. M., Gilmour, R. S., Neri, L. M., Manzoli, L., Corps, A. N., and Cocco, L. (1991) Mitogen-stimulated events in nuclei of Swiss 3T3 cells. Evidence for a direct link between changes of inositol lipids, protein kinase C requirement and the onset of DNA synthesis. *FEBS Lett.* **283**, 243–246
13. Kalasova, I., Faberova, V., Kalendova, A., Yildirim, S., Ulicna, L., Venit, T., and Hozak, P. (2016) Tools for visualization of phosphoinositides in the cell nucleus. *Histochem. Cell Biol.* **145**, 485–496
14. Vann, L. R., Wooding, F. B., Irvine, R. F., and Divecha, N. (1997) Metabolism and possible compartmentalization of inositol lipids in isolated rat-liver nuclei. *Biochem. J.* **327**(Pt 2), 569–576
15. Clarke, J. H., Letcher, A. J., D'Santos C, S., Halstead, J. R., Irvine, R. F., and Divecha, N. (2001) Inositol lipids are regulated during cell cycle progression in the nuclei of murine erythroleukaemia cells. *Biochem. J.* **357**, 905–910
16. Jones, D. R., Bultsma, Y., Keune, W. J., Halstead, J. R., Elouarrat, D., Mohammed, S., Heck, A. J., D'Santos, C. S., and Divecha, N. (2006) Nuclear PtdIns5P as a transducer of stress signaling: An *in vivo* role for PIP4Kbeta. *Mol. Cell* **23**, 685–695
17. Sarkes, D., and Rameh, L. E. (2010) A novel HPLC-based approach makes possible the spatial characterization of cellular PtdIns5P and other phosphoinositides. *Biochem. J.* **428**, 375–384
18. Gillooly, D. J., Morrow, I. C., Lindsay, M., Gould, R., Bryant, N. J., Gaullier, J. M., Parton, R. G., and Stenmark, H. (2000) Localization of phosphatidylinositol 3-phosphate in yeast and mammalian cells. *EMBO J.* **19**, 4577–4588
19. Lindsay, Y., McCoull, D., Davidson, L., Leslie, N., Fairservice, A., Gray, A., Lucocq, J., and Downes, C. (2006) Localization of agonist-sensitive PtdIns(3,4,5)P3 reveals a nuclear pool that is insensitive to PTEN expression. *J. Cell Sci.* **119**, 5160–5168
20. Boronenkov, I. V., Loijens, J. C., Umeda, M., and Anderson, R. A. (1998) Phosphoinositide signaling pathways in nuclei are associated with nuclear speckles containing pre-mRNA processing factors. *Mol. Biol. Cell* **9**, 3547–3560
21. Osborne, S. L., Thomas, C. L., Gschmeissner, S., and Schiavo, G. (2001) Nuclear PtdIns(4,5)P2 assembles in a mitotically regulated particle involved in pre-mRNA splicing. *J. Cell Sci.* **114**, 2501–2511
22. Watt, S. A., Kular, G., Fleming, I. N., Downes, C. P., and Lucocq, J. M. (2002) Subcellular localization of phosphatidylinositol 4,5-bisphosphate using the pleckstrin homology domain of phospholipase C delta1. *Biochem. J.* **363**, 657–666
23. Watt, S. A., Kimber, W. A., Fleming, I. N., Leslie, N. R., Downes, C. P., and Lucocq, J. M. (2004) Detection of novel intracellular agonist responsive pools of phosphatidylinositol 3,4-bisphosphate using the TAPP1 pleckstrin homology domain in immunoelectron microscopy. *Biochem. J.* **377**, 653–663
24. Kwon, I. S., Lee, K. H., Choi, J. W., and Ahn, J. Y. (2010) PI(3,4,5)P3 regulates the interaction between Akt and B23 in the nucleus. *BMB Rep.* **43**, 127–132

25. Karlsson, T., Altankhuyag, A., Dobrovolska, O., Turcu, D. C., and Lewis, A. E. (2016) A polybasic motif in ErbB3-binding protein 1 (EBP1) has key functions in nucleolar localization and polyphosphoinositide interaction. *Biochem. J.* **473**, 2033–2047
26. Faberova, V., Kalasova, I., Krausova, A., and Hozak, P. (2020) Super-resolution localisation of nuclear PI(4)P and identification of its interacting proteome. *Cells* **9**, 1191
27. Hoboth, P., Sztacho, M., Šebesta, O., Schätz, M., Castano, E., and Hozák, P. (2021) Nanoscale mapping of nuclear phosphatidylinositol phosphate landscape by dual-color dSTORM. *Biochim. Biophys. Acta Mol. Cell Biol. Lipids* **1866**, 158890
28. Mazloumi Gavgani, F., Karlsson, T., Tangen, I. L., Morovicz, A. P., Arnesen, V. S., Turcu, D. C., Ninzima, S., Spang, K., Krakstad, C., Guillermet-Guibert, J., and Lewis, A. E. (2021) Nuclear upregulation of class I phosphoinositide 3-kinase p110beta correlates with high 47S rRNA levels in cancer cells. *J. Cell Sci.* **134**, jcs246090
29. Blind, R. D., Sablin, E. P., Kuchenbecker, K. M., Chiu, H. J., Deacon, A. M., Das, D., Fletterick, R. J., and Ingraham, H. A. (2014) The signaling phospholipid PIP3 creates a new interaction surface on the nuclear receptor SF-1. *Proc. Natl. Acad. Sci. U. S. A.* **111**, 15054–15059
30. Blind, R. D., Suzawa, M., and Ingraham, H. A. (2012) Direct modification and activation of a nuclear receptor-PIP2 complex by the inositol lipid kinase IPMK. *Sci. Signal.* **5**, ra44
31. Sablin, E. P., Blind, R. D., Uthayaruban, R., Chiu, H. J., Deacon, A. M., Das, D., Ingraham, H. A., and Fletterick, R. J. (2015) Structure of liver receptor homolog-1 (NR5A2) with PIP3 hormone bound in the ligand binding pocket. *J. Struct. Biol.* **192**, 342–348
32. Layerenza, J. P., Gonzalez, P., Garcia de Bravo, M. M., Polo, M. P., Sisti, M. S., and Ves-Losada, A. (2013) Nuclear lipid droplets: A novel nuclear domain. *Biochim. Biophys. Acta* **1831**, 327–340
33. Romanauska, A., and Kohler, A. (2018) The inner nuclear membrane is a metabolically active territory that generates nuclear lipid droplets. *Cell* **174**, 700–715.e718
34. Sobol, M., Krausova, A., Yildirim, S., Kalasova, I., Faberova, V., Vrkoslav, V., Philimonenko, V., Marasek, P., Pastorek, L., Capek, M., Lubovska, Z., Ulicna, L., Tsuji, T., Lisa, M., Cvacka, J., *et al*. (2018) Nuclear phosphatidylinositol 4,5-bisphosphate islets contribute to efficient RNA polymerase II-dependent transcription. *J. Cell Sci.* **131**, jcs211094
35. Irvine, R. F. (2003) Nuclear lipid signalling. *Nat. Rev. Mol. Cell Biol.* **4**, 349–360
36. Okada, M., and Ye, K. (2009) Nuclear phosphoinositide signaling regulates messenger RNA export. *RNA Biol.* **6**, 12–16
37. Martelli, A. M., Ognibene, A., Buontempo, F., Fini, M., Bressanin, D., Goto, K., McCubrey, J. A., Cocco, L., and Evangelisti, C. (2011) Nuclear phosphoinositides and their roles in cell biology and disease. *Crit. Rev. Biochem. Mol. Biol.* **46**, 436–457
38. Viiri, K., Maki, M., and Lohi, O. (2012) Phosphoinositides as regulators of protein-chromatin interactions. *Sci. Signal.* **5**, pe19
39. Musille, P. M., Kohn, J. A., and Ortlund, E. A. (2013) Phospholipid–driven gene regulation. *FEBS Lett.* **587**, 1238–1246
40. Davis, W. J., Lehmann, P. Z., and Li, W. (2015) Nuclear PI3K signaling in cell growth and tumorigenesis. *Front. Cell Dev. Biol.* **3**, 24
41. Hamann, B. L., and Blind, R. D. (2018) Nuclear phosphoinositide regulation of chromatin. *J. Cell Physiol.* **233**, 107–123
42. Hu, Y., Liu, Z., and Ye, K. (2005) Phosphoinositol lipids bind to phosphatidylinositol 3 (PI3)-kinase enhancer GTPase and mediate its stimulatory effect on PI3-kinase and Akt signalings. *Proc. Natl. Acad. Sci. U. S. A.* **102**, 16853–16858
43. Tanaka, K., Horiguchi, K., Yoshida, T., Takeda, M., Fujisawa, H., Takeuchi, K., Umeda, M., Kato, S., Ihara, S., Nagata, S., and Fukui, Y. (1999) Evidence that a phosphatidylinositol 3,4,5-trisphosphate-binding protein can function in nucleus. *J. Biol. Chem.* **274**, 3919–3922
44. Gozani, O., Karuman, P., Jones, D. R., Ivanov, D., Cha, J., Lugovskoy, A. A., Baird, C. L., Zhu, H., Field, S. J., Lessnick, S. L., Villasenor, J., Mehrotra, B., Chen, J., Rao, V. R., Brugge, J. S., *et al*. (2003) The PHD finger of the chromatin-associated protein ING2 functions as a nuclear phosphoinositide receptor. *Cell* **114**, 99–111
45. Ahn, J. Y., Liu, X., Cheng, D., Peng, J., Chan, P. K., Wade, P. A., and Ye, K. (2005) Nucleophosmin/B23, a nuclear PI(3,4,5)P(3) receptor, mediates the antiapoptotic actions of NGF by inhibiting CAD. *Mol. Cell* **18**, 435–445
46. Kaadige, M. R., and Ayer, D. E. (2006) The polybasic region that follows the plant homeodomain zinc finger 1 of Pf1 is necessary and sufficient for specific phosphoinositide binding. *J. Biol. Chem.* **281**, 28831–28836
47. Okada, M., Jang, S. W., and Ye, K. (2008) Akt phosphorylation and nuclear phosphoinositide association mediate mRNA export and cell proliferation activities by ALY. *Proc. Natl. Acad. Sci. U. S. A.* **105**, 8649–8654
48. Viiri, K. M., Janis, J., Siggers, T., Heinonen, T. Y., Valjakka, J., Bulyk, M. L., Maki, M., and Lohi, O. (2009) DNA-binding and -bending activities of SAP30L and SAP30 are mediated by a zinc-dependent module and monophosphoinositides. *Mol. Cell. Biol.* **29**, 342–356
49. Lewis, A. E., Sommer, L., Arntzen, M. O., Strahm, Y., Morrice, N. A., Divecha, N., and D'Santos, C. S. (2011) Identification of nuclear phosphatidylinositol 4,5-bisphosphate-interacting proteins by neomycin extraction. *Mol. Cell. Proteomics* **10**. M110.003376
50. Bidlingmaier, S., Wang, Y., Liu, Y., Zhang, N., and Liu, B. (2011) Comprehensive analysis of yeast surface displayed cDNA library selection outputs by exon microarray to identify novel protein-ligand interactions. *Mol. Cell. Proteomics* **10**. M110.005116
51. Toska, E., Campbell, H. A., Shandilya, J., Goodfellow, S. J., Shore, P., Medler, K. F., and Roberts, S. G. (2012) Repression of transcription by WT1-BASP1 requires the myristoylation of BASP1 and the PIP2-dependent recruitment of histone deacetylase. *Cell Rep.* **2**, 462–469
52. Gelato, K. A., Tauber, M., Ong, M. S., Winter, S., Hiragami-Hamada, K., Sindlinger, J., Lemak, A., Bultsma, Y., Houliston, S., Schwarzer, D., Divecha, N., Arrowsmith, C. H., and Fischle, W. (2014) Accessibility of different histone H3-binding domains of UHRF1 is allosterically regulated by phosphatidylinositol 5-phosphate. *Mol. Cell* **54**, 905–919
53. Stijf-Bultsma, Y., Sommer, L., Tauber, M., Baalbaki, M., Giardoglou, P., Jones, D. R., Gelato, K. A., van Pelt, J., Shah, Z., Rahnamoun, H., Toma, C., Anderson, K. E., Hawkins, P., Lauberth, S. M., Haramis, A. P., *et al*. (2015) The basal transcription complex component TAF3 transduces changes in nuclear phosphoinositides into transcriptional output. *Mol. Cell* **58**, 453–467
54. Kostrhon, S., Kontaxis, G., Kaufmann, T., Schirghuber, E., Kubicek, S., Konrat, R., and Slade, D. (2017) A histone-mimicking interdomain linker in a multi-domain protein modulates multivalent histone binding. *J. Biol. Chem.* **292**, 17643–17657
55. Ulicna, L., Kalendova, A., Kalasova, I., Vacik, T., and Hozak, P. (2018) PIP2 epigenetically represses rRNA genes transcription interacting with PHF8. *Biochim. Biophys. Acta* **1863**, 266–275
56. Tabellini, G., Bortul, R., Santi, S., Riccio, M., Baldini, G., Cappellini, A., Billi, A. M., Berezney, R., Ruggeri, A., Cocco, L., and Martelli, A. M. (2003) Diacylglycerol kinase-theta is localized in the speckle domains of the nucleus. *Exp. Cell Res.* **287**, 143–154
57. Mellman, D. L., Gonzales, M. L., Song, C., Barlow, C. A., Wang, P., Kendziorski, C., and Anderson, R. A. (2008) A PtdIns4,5P2-regulated nuclear poly(A) polymerase controls expression of select mRNAs. *Nature* **451**, 1013–1017
58. Zhao, K., Wang, W., Rando, O. J., Xue, Y., Swiderek, K., Kuo, A., and Crabtree, G. R. (1998) Rapid and phosphoinositol-dependent binding of the SWI/SNF-like BAF complex to chromatin after T lymphocyte receptor signaling. *Cell* **95**, 625–636
59. Rando, O. J., Zhao, K., Janmey, P., and Crabtree, G. R. (2002) Phosphatidylinositol-dependent actin filament binding by the SWI/SNF-like BAF chromatin remodeling complex. *Proc. Natl. Acad. Sci. U. S. A.* **99**, 2824–2829
60. Yu, H., Fukami, K., Watanabe, Y., Ozaki, C., and Takenawa, T. (1998) Phosphatidylinositol 4,5-bisphosphate reverses the inhibition of RNA transcription caused by histone H1. *Eur. J. Biochem.* **251**, 281–287
61. Choi, S., Chen, M., Cryns, V. L., and Anderson, R. A. (2019) A nuclear phosphoinositide kinase complex regulates p53. *Nat. Cell Biol.* **21**, 462–475
62. Yildirim, S., Castano, E., Sobol, M., Philimonenko, V. V., Dzijak, R., Venit, T., and Hozak, P. (2013) Involvement of phosphatidylinositol 4,5-bisphosphate in RNA polymerase I transcription. *J. Cell Sci.* **126**, 2730–2739
63. Sobol, M., Yildirim, S., Philimonenko, V. V., Marasek, P., Castano, E., and Hozak, P. (2013) UBF complexes with phosphatidylinositol 4,5-bisphosphate in nucleolar organizer regions regardless of ongoing RNA polymerase I activity. *Nucleus* **4**, 478–486
64. Alvarez-Venegas, R., Sadder, M., Hlavacka, A., Baluska, F., Xia, Y., Lu, G., Firsov, A., Sarath, G., Moriyama, H., Dubrovsky, J. G., and Avramova, Z.

(2006) The Arabidopsis homolog of trithorax, ATX1, binds phosphatidylinositol 5-phosphate, and the two regulate a common set of target genes. *Proc. Natl. Acad. Sci. U. S. A.* **103**, 6049–6054
65. Marques, M., Kumar, A., Poveda, A. M., Zuluaga, S., Hernandez, C., Jackson, S., Pasero, P., and Carrera, A. C. (2009) Specific function of phosphoinositide 3-kinase beta in the control of DNA replication. *Proc. Natl. Acad. Sci. U. S. A.* **106**, 7525–7530
66. Kumar, A., Fernandez-Capetillo, O., and Carrera, A. C. (2010) Nuclear phosphoinositide 3-kinase beta controls double-strand break DNA repair. *Proc. Natl. Acad. Sci. U. S. A.* **107**, 7491–7496
67. Yang, X., Ongusaha, P. P., Miles, P. D., Havstad, J. C., Zhang, F., So, W. V., Kudlow, J. E., Michell, R. H., Olefsky, J. M., Field, S. J., and Evans, R. M. (2008) Phosphoinositide signalling links O-GlcNAc transferase to insulin resistance. *Nature* **451**, 964–969
68. Catimel, B., Yin, M. X., Schieber, C., Condron, M., Patsiouras, H., Catimel, J., Robinson, D. E., Wong, L. S., Nice, E. C., Holmes, A. B., and Burgess, A. W. (2009) PI(3,4,5)P3 interactome. *J. Proteome Res.* **8**, 3712–3726
69. Krugmann, S., Anderson, K. E., Ridley, S. H., Risso, N., McGregor, A., Coadwell, J., Davidson, K., Eguinoa, A., Ellson, C. D., Lipp, P., Manifava, M., Ktistakis, N., Painter, G., Thuring, J. W., Cooper, M. A., *et al*. (2002) Identification of ARAP3, a novel PI3K effector regulating both Arf and Rho GTPases, by selective capture on phosphoinositide affinity matrices. *Mol. Cell* **9**, 95–108
70. Rowland, M. M., Bostic, H. E., Gong, D., Speers, A. E., Lucas, N., Cho, W., Cravatt, B. F., and Best, M. D. (2011) Phosphatidylinositol 3,4,5-trisphosphate activity probes for the labeling and proteomic characterization of protein binding partners. *Biochemistry* **50**, 11143–11161
71. Jungmichel, S., Sylvestersen, K. B., Choudhary, C., Nguyen, S., Mann, M., and Nielsen, M. L. (2014) Specificity and commonality of the phosphoinositide-binding proteome analyzed by quantitative mass spectrometry. *Cell Rep.* **6**, 578–591
72. Jarboui, M. A., Wynne, K., Elia, G., Hall, W. W., and Gautier, V. W. (2011) Proteomic profiling of the human T-cell nucleolus. *Mol. Immunol.* **49**, 441–452
73. Hassa, P. O., Haenni, S. S., Buerki, C., Meier, N. I., Lane, W. S., Owen, H., Gersbach, M., Imhof, R., and Hottiger, M. O. (2005) Acetylation of poly(ADP-ribose) polymerase-1 by p300/CREB-binding protein regulates coactivation of NF-kappaB-dependent transcription. *J. Biol. Chem.* **280**, 40450–40464
74. Mohammed, H., D'Santos, C., Serandour, A. A., Ali, H. R., Brown, G. D., Atkins, A., Rueda, O. M., Holmes, K. A., Theodorou, V., Robinson, J. L., Zwart, W., Saadi, A., Ross-Innes, C. S., Chin, S. F., Menon, S., *et al*. (2013) Endogenous purification reveals GREB1 as a key estrogen receptor regulatory factor. *Cell Rep.* **3**, 342–349
75. Mi, H., Muruganujan, A., and Thomas, P. D. (2013) PANTHER in 2013: Modeling the evolution of gene function, and other gene attributes, in the context of phylogenetic trees. *Nucleic Acids Res.* **41**, D377–D386
76. Thomas, P. D., Campbell, M. J., Kejariwal, A., Mi, H., Karlak, B., Daverman, R., Diemer, K., Muruganujan, A., and Narechania, A. (2003) Panther: A library of protein families and subfamilies indexed by function. *Genome Res.* **13**, 2129–2141
77. Szklarczyk, D., Morris, J. H., Cook, H., Kuhn, M., Wyder, S., Simonovic, M., Santos, A., Doncheva, N. T., Roth, A., Bork, P., Jensen, L. J., and von Mering, C. (2017) The STRING database in 2017: Quality-controlled protein-protein association networks, made broadly accessible. *Nucleic Acids Res.* **45**, D362–D368
78. Perez-Riverol, Y., Csordas, A., Bai, J., Bernal-Llinares, M., Hewapathirana, S., Kundu, D. J., Inuganti, A., Griss, J., Mayer, G., Eisenacher, M., Perez, E., Uszkoreit, J., Pfeuffer, J., Sachsenberg, T., Yilmaz, S., *et al*. (2019) The PRIDE database and related tools and resources in 2019: Improving support for quantification data. *Nucleic Acids Res.* **47**, D442–D450
79. Klarlund, J. K., Guilherme, A., Holik, J. J., Virbasius, J. V., Chawla, A., and Czech, M. P. (1997) Signaling by phosphoinositide-3,4,5-trisphosphate through proteins containing pleckstrin and Sec7 homology domains. *Science* **275**, 1927–1930
80. Ferguson, K. M., Kavran, J. M., Sankaran, V. G., Fournier, E., Isakoff, S. J., Skolnik, E. Y., and Lemmon, M. A. (2000) Structural basis for discrimination of 3-phosphoinositides by pleckstrin homology domains. *Mol. Cell* **6**, 373–384
81. Manna, D., Albanese, A., Park, W. S., and Cho, W. (2007) Mechanistic basis of differential cellular responses of phosphatidylinositol 3,4-bisphosphate- and phosphatidylinositol 3,4,5-trisphosphate-binding pleckstrin homology domains. *J. Biol. Chem.* **282**, 32093–32105
82. Guillou, H., Lecureuil, C., Anderson, K. E., Suire, S., Ferguson, G. J., Ellson, C. D., Gray, A., Divecha, N., Hawkins, P. T., and Stephens, L. R. (2007) Use of the GRP1 PH domain as a tool to measure the relative levels of PtdIns(3,4,5)P3 through a protein-lipid overlay approach. *J. Lipid Res.* **48**, 726–732
83. Schacht, J. (1976) Inhibition by neomycin of polyphosphoinositide turnover in subcellular fractions of Guinea-pig cerebral cortex *in vitro*. *J. Neurochem.* **27**, 1119–1124
84. Schacht, J. (1978) Purification of polyphosphoinositides by chromatography on immobilized neomycin. *J. Lipid Res.* **19**, 1063–1067
85. Schacht, J. (1979) Isolation of an aminoglycoside receptor from Guinea pig inner ear tissues and kidney. *Arch. Otorhinolaryngol.* **224**, 129–134
86. Dixon, M. J., Gray, A., Schenning, M., Agacan, M., Tempel, W., Tong, Y., Nedyalkova, L., Park, H. W., Leslie, N. R., van Aalten, D. M., Downes, C. P., and Batty, I. H. (2012) IQGAP proteins reveal an atypical phosphoinositide (aPI) binding domain with a pseudo C2 domain fold. *J. Biol. Chem.* **287**, 22483–22496
87. Salim, K., Bottomley, M. J., Querfurth, E., Zvelebil, M. J., Gout, I., Scaife, R., Margolis, R. L., Gigg, R., Smith, C. I., Driscoll, P. C., Waterfield, M. D., and Panayotou, G. (1996) Distinct specificity in the recognition of phosphoinositides by the pleckstrin homology domains of dynamin and Bruton's tyrosine kinase. *EMBO J.* **15**, 6241–6250
88. Zheng, J., Cahill, S. M., Lemmon, M. A., Fushman, D., Schlessinger, J., and Cowburn, D. (1996) Identification of the binding site for acidic phospholipids on the pH domain of dynamin: Implications for stimulation of GTPase activity. *J. Mol. Biol.* **255**, 14–21
89. Ivarsson, Y., Wawrzyniak, A. M., Kashyap, R., Polanowska, J., Betzi, S., Lembo, F., Vermeiren, E., Chiheb, D., Lenfant, N., Morelli, X., Borg, J. P., Reboul, J., and Zimmermann, P. (2013) Prevalence, specificity and determinants of lipid-interacting PDZ domains from an in-cell screen and *in vitro* binding experiments. *PLoS One* **8**, e54581
90. Scott, M. S., Troshin, P. V., and Barton, G. J. (2011) NoD: A nucleolar localization sequence detector for eukaryotic and viral proteins. *BMC Bioinformatics* **12**, 317
91. Calkins, A. S., Iglehart, J. D., and Lazaro, J. B. (2013) DNA damage-induced inhibition of rRNA synthesis by DNA-PK and PARP-1. *Nucleic Acids Res.* **41**, 7378–7386
92. Meder, V. S., Boeglin, M., de Murcia, G., and Schreiber, V. (2005) PARP-1 and PARP-2 interact with nucleophosmin/B23 and accumulate in transcriptionally active nucleoli. *J. Cell Sci.* **118**, 211–222
93. Engbrecht, M., and Mangerich, A. (2020) The nucleolus and PARP1 in cancer biology. *Cancers (Basel)* **12**, 1813
94. Barlow, C. A., Laishram, R. S., and Anderson, R. A. (2010) Nuclear phosphoinositides: A signaling enigma wrapped in a compartmental conundrum. *Trends Cell Biol.* **20**, 25–35
95. Fiume, R., Keune, W. J., Faenza, I., Bultsma, Y., Ramazzotti, G., Jones, D. R., Martelli, A. M., Somner, L., Follo, M. Y., Divecha, N., and Cocco, L. (2012) Nuclear phosphoinositides: Location, regulation and function. *Subcell Biochem.* **59**, 335–361
96. Shah, Z. H., Jones, D. R., Sommer, L., Foulger, R., Bultsma, Y., D'Santos, C., and Divecha, N. (2013) Nuclear phosphoinositides and their impact on nuclear functions. *FEBS J.* **280**, 6295–6310
97. Kakuk, A., Friedlander, E., Vereb, G., Jr., Kasa, A., Balla, A., Balla, T., Heilmeyer, L. M., Jr., Gergely, P., and Vereb, G. (2006) Nucleolar localization of phosphatidylinositol 4-kinase PI4K230 in various mammalian cells. *Cytometry A* **69**, 1174–1183
98. Chakrabarti, R., Sanyal, S., Ghosh, A., Bhar, K., Das, C., and Siddhanta, A. (2015) Phosphatidylinositol-4-phosphate 5-kinase 1alpha modulates ribosomal RNA gene silencing through its interaction with histone H3 lysine 9 trimethylation and heterochromatin protein HP1-alpha. *J. Biol. Chem.* **290**, 20893–20903
99. Ehm, P., Nalaskowski, M. M., Wundenberg, T., and Jucker, M. (2015) The tumor suppressor SHIP1 colocalizes in nucleolar cavities with p53 and components of PML nuclear bodies. *Nucleus* **6**, 154–164
100. Li, P., Wang, D., Li, H., Yu, Z., Chen, X., and Fang, J. (2014) Identification of nucleolus-localized PTEN and its function in regulating ribosome biogenesis. *Mol. Biol. Rep.* **41**, 6383–6390
101. Irvine, R. F. (2006) Nuclear inositide signalling – expansion, structures and clarification. *Biochim. Biophys. Acta* **1761**, 505–508
102. Klein, D. E., Lee, A., Frank, D. W., Marks, M. S., and Lemmon, M. A. (1998) The pleckstrin homology domains of dynamin isoforms require

oligomerization for high affinity phosphoinositide binding. *J. Biol. Chem.* **273**, 27725–27733
103. Boisvert, F. M., Ahmad, Y., Gierlinski, M., Charriere, F., Lamont, D., Scott, M., Barton, G., and Lamond, A. I. (2012) A quantitative spatial proteomics analysis of proteome turnover in human cells. *Mol. Cell. Proteomics* **11**. M111.011429
104. Johnson, M., Sharma, M., Brocardo, M. G., and Henderson, B. R. (2011) IQGAP1 translocates to the nucleus in early S-phase and contributes to cell cycle progression after DNA replication arrest. *Int. J. Biochem. Cell Biol.* **43**, 65–73
105. Hammond, G. R., Fischer, M. J., Anderson, K. E., Holdich, J., Koteci, A., Balla, T., and Irvine, R. F. (2012) PI4P and PI(4,5)P2 are essential but independent lipid determinants of membrane identity. *Science* **337**, 727–730
106. Heo, W. D., Inoue, T., Park, W. S., Kim, M. L., Park, B. O., Wandless, T. J., and Meyer, T. (2006) PI(3,4,5)P3 and PI(4,5)P2 lipids target proteins with polybasic clusters to the plasma membrane. *Science* **314**, 1458–1461
107. Deleris, P., Bacqueville, D., Gayral, S., Carrez, L., Salles, J. P., Perret, B., and Breton-Douillon, M. (2003) SHIP-2 and PTEN are expressed and active in vascular smooth muscle cell nuclei, but only SHIP-2 is associated with nuclear speckles. *J. Biol. Chem.* **278**, 38884–38891
108. Elong Edimo, W., Derua, R., Janssens, V., Nakamura, T., Vanderwinden, J. M., Waelkens, E., and Erneux, C. (2011) Evidence of SHIP2 Ser132 phosphorylation, its nuclear localization and stability. *Biochem. J.* **439**, 391–401
109. Didichenko, S. A., and Thelen, M. (2001) Phosphatidylinositol 3-kinase c2alpha contains a nuclear localization sequence and associates with nuclear speckles. *J. Biol. Chem.* **276**, 48135–48142
110. Ulicna, L., Kalendova, A., Kalasova, I., Vacik, T., and Hozak, P. (2018) PIP2 epigenetically represses rRNA genes transcription interacting with PHF8. *Biochim. Biophys. Acta Mol. Cell Biol. Lipids* **1863**, 266–275
111. Viiri, K. M., Korkeamaki, H., Kukkonen, M. K., Nieminen, L. K., Lindfors, K., Peterson, P., Maki, M., Kainulainen, H., and Lohi, O. (2006) SAP30L interacts with members of the Sin3A corepressor complex and targets Sin3A to the nucleolus. *Nucleic Acids Res.* **34**, 3288–3298
112. Rancourt, A., and Satoh, M. S. (2009) Delocalization of nucleolar poly(-ADP-ribose) polymerase-1 to the nucleoplasm and its novel link to cellular sensitivity to DNA damage. *DNA Repair (Amst.)* **8**, 286–297
113. Brodska, B., Holoubek, A., Otevrelova, P., and Kuzelova, K. (2016) Low-dose actinomycin-D induces redistribution of wild-type and mutated nucleophosmin followed by cell death in leukemic cells. *J. Cell Biochem.* **117**, 1319–1329
114. Jordan, P., Mannervik, M., Tora, L., and Carmo-Fonseca, M. (1996) *In vivo* evidence that TATA-binding protein/SL1 colocalizes with UBF and RNA polymerase I when rRNA synthesis is either active or inactive. *J. Cell Biol.* **133**, 225–234
115. Boisvert, F. M., van Koningsbruggen, S., Navascues, J., and Lamond, A. I. (2007) The multifunctional nucleolus. *Nat. Rev. Mol. Cell Biol.* **8**, 574–585
116. Ogawa, L. M., and Baserga, S. J. (2017) Crosstalk between the nucleolus and the DNA damage response. *Mol. Biosyst.* **13**, 443–455
117. Scott, D. D., and Oeffinger, M. (2016) Nucleolin and nucleophosmin: Nucleolar proteins with multiple functions in DNA repair. *Biochem. Cell Biol.* **94**, 419–432
118. Boamah, E. K., Kotova, E., Garabedian, M., Jarnik, M., and Tulin, A. V. (2012) Poly(ADP-Ribose) polymerase 1 (PARP-1) regulates ribosomal biogenesis in Drosophila nucleoli. *PLoS Genet.* **8**, e1002442
119. Box, J. K., Paquet, N., Adams, M. N., Boucher, D., Bolderson, E., O'Byrne, K. J., and Richard, D. J. (2016) Nucleophosmin: From structure and function to disease development. *BMC Mol. Biol.* **17**, 19
120. Wang, Y. H., Hariharan, A., Bastianello, G., Toyama, Y., Shivashankar, G. V., Foiani, M., and Sheetz, M. P. (2017) DNA damage causes rapid accumulation of phosphoinositides for ATR signaling. *Nat. Commun.* **8**, 2118
121. Radons, J. (2016) The human HSP70 family of chaperones: Where do we stand? *Cell Stress Chaperones* **21**, 379–404
122. Sawarkar, R., and Paro, R. (2013) Hsp90@chromatin.nucleus: An emerging hub of a networker. *Trends Cell Biol.* **23**, 193–201
123. Kotoglou, P., Kalaitzakis, A., Vezyraki, P., Tzavaras, T., Michalis, L. K., Dantzer, F., Jung, J. U., and Angelidis, C. (2009) Hsp70 translocates to the nuclei and nucleoli, binds to XRCC1 and PARP-1, and protects HeLa cells from single-strand DNA breaks. *Cell Stress Chaperones* **14**, 391–406
124. Frottin, F., Schueder, F., Tiwary, S., Gupta, R., Korner, R., Schlichthaerle, T., Cox, J., Jungmann, R., Hartl, F. U., and Hipp, M. S. (2019) The nucleolus functions as a phase-separated protein quality control compartment. *Science* **365**, 342–347
125. Dubrez, L., Causse, S., Borges Bonan, N., Dumetier, B., and Garrido, C. (2020) Heat-shock proteins: Chaperoning DNA repair. *Oncogene* **39**, 516–529
126. Tao, Z., Gao, P., Hoffman, D. W., and Liu, H. W. (2008) Domain C of human poly(ADP-ribose) polymerase-1 is important for enzyme activity and contains a novel zinc-ribbon motif. *Biochemistry* **47**, 5804–5813